The DNA sequence of human chromosome 21

The chromosome 21 mapping and sequencing consortium

M. Hattori*¶¶, A. Fujiyama*, T. D. Taylor*, H. Watanabe*, T. Yada*, H.-S. Park*, A. Toyoda*, K. Ishii*, Y. Totoki*, D.-K. Choi*, E. Soeda†, M. Ohki‡, T. Takagi§, Y. Sakaki*§; S. Taudien‖¶¶, K. Blechschmidt‖, A. Polley‖, U. Menzel‖, J. Delabar¶, K. Kumpf‖, R. Lehmann‖, D. Patterson#, K. Reichwald‖, A. Rump‖, M. Schillhabel‖, A. Schudy‖, W. Zimmermann‖, A. Rosenthal‖; J. Kudoh☆¶¶, K. Shibuya☆, K. Kawasaki☆, S. Asakawa☆, A. Shintani☆, T. Sasaki☆, K. Nagamine☆, S. Mitsuyama☆, S. E. Antonarakis, S. Minoshima☆, N. Shimizu☆; G. Nordsiek††¶¶, K. Hornischer††, P. Brandt††, M. Scharfe††, O. Schön††, A. Desario‡‡, J. Reichelt††, G. Kauer††, H. Blöcker††; J. Ramser§§¶¶, A. Beck§§, S. Klages§§, S. Hennig§§, L. Riesselmann§§, E. Dagand§§, S. Wehrmeyer§§, K. Borzym§§, K. Gardiner#, D. Nizetic‖‖, F. Francis§§, H. Lehrach§§, R. Reinhardt§§ & M.-L. Yaspo§§**

Consortium Institutions:
* *RIKEN, Genomic Sciences Center, Sagamihara 228-8555, Japan*
‖ *Institut für Molekulare Biotechnologie, Genomanalyse, D-07745 Jena, Germany*
☆ *Department of Molecular Biology, Keio University School of Medicine, Tokyo 160-8582, Japan*
†† *GBF (German Research Centre for Biotechnology), Genome Analysis, D-38124 Braunschweig, Germany*
§§ *Max-Planck-Institut für Molekulare Genetik, D-14195 Berlin-Dahlem, Germany*
Collaborating Institutions:
† *RIKEN, Life Science Tsukuba Research Center, Tsukuba 305-0074, Japan*
‡ *Cancer Genomics Division, National Cancer Center Research Institute, Tokyo 104-0045, Japan*
§ *Human Genome Center, Institute of Medical Science, University of Tokyo, Tokyo 108-8639, Japan*
¶ *UMR 8602 CNRS, UFR Necker Enfants-Malades, Paris, 75730, France*
# *Eleanor Roosevelt Institute, Denver, Colorado 80206, USA*
** *Medical Genetics Division, University of Geneva Medical School, Geneva 1211, Switzerland*
‡‡ *CNRS UPR 1142, Institut de Biologie, Montpellier, 34060, France*
‖‖ *School of Pharmacy, University of London, London WC1N 1AX, UK*
¶¶ *These authors contributed equally to this work*

Chromosome 21 is the smallest human autosome. An extra copy of chromosome 21 causes Down syndrome, the most frequent genetic cause of significant mental retardation, which affects up to 1 in 700 live births. Several anonymous loci for monogenic disorders and predispositions for common complex disorders have also been mapped to this chromosome, and loss of heterozygosity has been observed in regions associated with solid tumours. Here we report the sequence and gene catalogue of the long arm of chromosome 21. We have sequenced 33,546,361 base pairs (bp) of DNA with very high accuracy, the largest contig being 25,491,867 bp. Only three small clone gaps and seven sequencing gaps remain, comprising about 100 kilobases. Thus, we achieved 99.7% coverage of 21q. We also sequenced 281,116 bp from the short arm. The structural features identified include duplications that are probably involved in chromosomal abnormalities and repeat structures in the telomeric and pericentromeric regions. Analysis of the chromosome revealed 127 known genes, 98 predicted genes and 59 pseudogenes.

Chromosome 21 represents around 1–1.5% of the human genome. Since the discovery in 1959 that Down syndrome occurs when there are three copies of chromosome 21 (ref. 1), about twenty disease loci have been mapped to its long arm, and the chromosome's structure and gene content have been intensively studied. Consequently, chromosome 21 was the first autosome for which a dense linkage map[2], yeast artificial chromosome (YAC) physical maps[3–6] and a *Not*I restriction map[7] were developed. The size of the long arm of the chromosome (21q) was estimated to be around 38 megabases (Mb), based on pulsed-field gel electrophoresis (PFGE) studies using *Not*I restriction fragments[7]. By 1995, when the sequencing effort was initiated, around 60 messenger RNAs specific to chromosome 21 had been characterized. Here we report and discuss the sequence and gene catalogue of the long arm of chromosome 21.

Chromosome geography

Mapping. We converted the euchromatic part of chromosome 21 into a minimum tiling path of 518 large-insert bacterial clones. This collection comprises 192 bacterial artificial chromosomes (BACs), 111 P1 artificial chromosomes (PACs), 101 P1, 81 cosmids, 33 fosmids and 5 polymerase chain reaction (PCR) products (Fig. 1). We used clones originating from four whole-genome libraries and nine chromosome-21-specific libraries. The latter were particularly useful for mapping the centromeric and telomeric repeat-containing regions and sequences showing homology with other human chromosomes.

We used two strategies to construct the sequence-ready map of chromosome 21. In the first, we isolated clones from arrayed genomic libraries by large-scale non-isotopic hybridization[8]. We built primary contigs from hybridization data assembled by simulated annealing, and refined clone overlaps by restriction digest fingerprinting. Contigs were anchored onto PFGE maps of *Not*I restriction fragments and ordered using known sequence tag site (STS) framework markers. We used metaphase fluorescent *in situ* hybridization (FISH) to check the locations of more than 250 clones. The integrity of the contigs was confirmed by FISH, and gaps were sized by a combination of fibre FISH and interphase nuclei mapping. Gaps were filled by multipoint clone walking. In the second strategy, we isolated seed clones using selected STS markers and then either end-sequenced or partially sequenced them at fivefold redundancy. Seed clones were extended in both directions with new genomic clones, which were identified either by PCR using amplimers derived from parental clone ends or by sequence searches of the BAC end sequence database (http://www.tigr.org). Nascent contigs were confirmed by sequence comparison.

The final map is shown in Fig. 1. It comprises 518 bacterial

clones forming four large contigs. Three small clone gaps remain despite screening of all available libraries. The estimated sizes of these gaps are 40, 30 and 30 kilobases (kb), respectively, as indicated by fibre FISH (see supporting data set, last section (http://chr21.r2-berlin.mpg.de).

Sequencing. We used two sequencing strategies. In the first, large-insert clones were shotgun cloned into M13 or plasmid vectors. DNA of subclones was prepared or amplified, and then sequenced using dye terminator and dye primer chemistry. On average, clones were sequenced at 8–10-fold redundancy. In the second approach, we sequenced large-insert clones using a nested deletion method[9]. The redundancy of the nested deletion method was about fourfold. Gaps were closed by a combination of nested deletions, long reads, reverse reads, sequence walks on shotgun clones and large insert clones using custom primers. Some gaps were also closed by sequencing PCR products.

The total length of the sequenced parts of the long arm of chromosome 21 is 33,546,361 bp. The sequence extends from a 25-kb stretch of α-satellite repeats near the centromere to the telomeric repeat array. Seven sequencing gaps remain, totalling less than 3 kb. The largest contig spans 25.5 Mb on 21q. The total length of 21q, including the three clone gaps, is about 33.65 Mb. Thus, we achieved 99.7% coverage of the chromosome. We also sequenced a small contig of 281,116 bp on the p arm of chromosome 21.

We estimated the accuracy of the final sequence by comparing 18 overlapping sequence portions spanning 1.2 Mb. We estimate from this external checking exercise that the accuracy of the entire sequence exceeds 99.995%.

Sequence variations. Twenty-two overlapping sequence portions comprising 1.36 Mb and spread over the entire chromosome were compared for sequence variations and small deletions or insertions. We detected 1,415 nucleotide variations and 310 small deletions or insertions and confirmed them by inspecting trace files. There was an average of one sequence difference for each 787 bp, but the observed sequence variations were not evenly distributed along 21q. In the telomeric portion (21q22.3–qter) the average was one difference for each 500 bp. The highest sequence variation (one difference in 400 bp) was found in a 98-kb segment from this region. In the proximal portion (21q11–q22.3) we found on average one difference per 1,000 bp; the lowest level was 1 in 3,600 bp in a 61-kb segment of 21q22.1.

Interspersed repeats. Table 1 summarizes the repeat content of chromosome 21. Chromosome 21 contains 9.48% Alu sequences and 12.93% LINE1 elements, in contrast with chromosome 22 which contains 16.8% Alu and 9.73% LINE1 sequences[10].

Table 1 The content of interspersed repeats in human chromosome 21

Repeat type	Total number of elements	Coverage (bp)	Coverage (%)
SINEs	15,748	3,667,752	10.84%
ALUs	12,341	3,208,437	9.48%
MIRs	3,407	459,315	1.36%
LINEs	12,723	5,245,516	15.51%
LINE1	8,982	4,372,851	12.93%
LINE2	3,741	872,665	2.58%
LTR elements	9,598	3,116,881	9.21%
MaLRs	5,379	1,646,297	4.87%
Retroviral	2,115	760,119	2.25%
MER4 group	1,396	479,451	1.42%
Other LTR	708	231,014	0.68%
DNA elements	3,950	812,031	2.40%
MER1 type	2,553	460,769	1.36%
MER2 type	851	257,653	0.76%
Mariners	168	26,235	0.08%
Other DNA elements	378	67,374	0.20%
Unclassified	64	15,234	0.05%
Total interspersed repeats	42,083	12,857,414	38.01%
Simple repeats	5,987	427,755	1.26%
Low complexity	5,868	249,449	0.74%
Total	54,045	13,551,271	40.06%
Total sequence length	33,827,477		
G+C%	40.89%		

Figure 1 The sequence map of human chromosome 21. Sequence positions are indicated in Mb. Annotated features are shown by coloured boxes and lines. The chromosome is oriented with the short p-arm to the left and the long q-arm to the right. Vertical grey box, centromere. The three small clone gaps are indicated by narrow grey vertical boxes (in proportion to estimated size) on the right of the q-arm. The cytogenetic map was drawn by simple linear stretching of the ISCN 850-band, Giemsa-stained ideogram to match the length of the sequence: the boundaries are only indicative and are not supported by experimental evidence. In the mapping phase, information on STS markers was collected from publicly available resources. The progress of mapping and sequencing was monitored using a sequence data repository in which sequences of each clone were aligned according to their map positions. A unified map of these markers was automatically generated (http://hgp.gsc.riken.go.jp/marker/) and enabled us to carry out simultaneous sequencing and library screening among centres. Vertical lines: markers, according to sequence position, from GDB (black; http://www.gdb.org/), the GB4 radiation hybrid map (blue; Whitehead Institute, Massachusetts Institute of Technology)[43], the G3 radiation hybrid map (dark green; Stanford Human Genome Centre, California)[44] and two linkage maps (red; Genethon; CHLC)[45,46]. Only marker distribution is presented here: additional details, such as marker names and positions, can be found on our web sites. The *Not*I physical map of chromosome 21 was also used[7] (*Not*I sites, light green). Genes are indicated as boxes or lines according to strand along the upper scale in three categories: known genes (category 1, red), predicted genes (categories 2 and 3, light green; category 4, light blue) and pseudogenes (category 5, violet). For genes of categories 1, 2, 3 and 5, the approved symbols from the HUGO nomenclature committee are used. CpG islands are olive (they were identified when they exceeded 400 bp in length, contained more than 55% GC, showed an observed over expected CpG frequency of >0.6 and had no match to repetitive sequences).The G+C content is shown as a graph in the middle of the Figure. It was calculated on the basis of the number of G and C nucleotides in a 100-kb sliding window in 1-kb steps across the sequence. The clone contig consists of all clones that were sequenced to 'finished' quality from all five centres in the consortium. Clones are indicated as coloured boxes by centre: red, RIKEN; dark blue, IMB; light blue, Keio; yellow, GBF; and green, MPIMG. Clones that were only partially sequenced have grey boxes on either end to show the actual or estimated clone end position. Four whole-genome libraries (RPCI-11 BAC, Keio BAC, Caltech BAC and RPCI1, 3-5 PAC) and nine chromosome-specific libraries (CMB21-BAC, Roizes-BAC, CMP21-P1, CMC21-cosmid, LLNCO21, KU21D, ICRFc102 and ICRFc103 cosmid, and CMF21-fosmid) were used to isolate clones (see http://hgp.gsc.riken.go.jp or http://chr21.rz-berlin.mpg.de for library information). Breakpoints from chromosomal rearrangements are shown as coloured boxes according to their classification: natural (green), spontaneously occurring in cell lines (yellow), radiation induced (purple) and combinations of the above (black). Blue boxes, intra-chromosomal duplications; green boxes, inter-chromosomal duplications (see text). Alu (red) and LINE1 (blue) interspersed repeat element densities are shown in the bottom graph as the percentage of the sequence using the same method of calculation as for G+C content. The final non-redundant sequence was divided into 340-kb segments (grey boxes), with 1-kb overlaps (to avoid splitting of most exons in both segments), and has been registered, along with biological annotations, in the DDBJ/EMBL/GenBank databases under accession numbers AP001656–AP001761 (DDBJ) and AL163201–AL163306 (EMBL). Segments for the three clone gaps (accession numbers AP001742/AL163287, AP001744/AL163289 and AP001750/AL163295) have also been deposited in the databases with a number of Ns corresponding to the estimated gap lengths. The sequences and additional information can be found from the home pages of the participating centres of the chromosome 21 sequencing consortium (RIKEN, http://hgp.gsc.riken.go.jp/; IMB, http://genome.imb-jena.de/; Keio, http://adenine.dmb.med.keio.ac.jp/; GBF, http://www.genome.gbf.de/; MPI, http://chr21.rz-berlin.mpg.de/).

Gene catalogue

The gene catalogue of chromosome 21 contains known genes, novel putative genes predicted *in silico* from genomic sequence analysis and pseudogenes. The catalogue was arbitrarily divided into five main hierarchical categories (see below) to distinguish known genes from pure gene predictions, and also anonymous complementary DNA sequences from those exhibiting similarities to known proteins or modular domains.

The criteria governing the gene classification were based on the results of the integrated results of computational analysis using exon prediction programs and sequence similarity searches. We applied the following parameters: (1) Putative coding exons were predicted using GRAIL, GENSCAN and MZEF programs. Consistent exons were defined as those that were predicted by at least two programs. (2) Nucleotide sequence identities to expressed sequence tags (ESTs) (as identified by using BlastN with default parameters) were considered as a hallmark for gene prediction only if these ESTs were spliced into two or more exons in genomic DNA, and showed greater than 95% identity over the matched region. These criteria are conservative and were chosen to discard spurious matches arising from either cDNAs primed from intronic sites or repetitive elements frequently found in 5′ or 3′ untranslated regions. (3) Amino-acid similarities to known proteins or modular functional domains were considered to be significant when an overall identity of greater than 25% over more than 50 amino-acid residues was observed (as detected using BlastX with Blossum 62 matrix against the non-redundant database).

Gene categories. The results of sequence analysis were visually inspected to locate known genes, to identify new genes and to unravel novel putative transcription units after assembling consistent predicted exons into so-called *in silico* gene models. These gene predictions were also evaluated by incorporating information provided by EST and protein matches. Each gene was assigned to one of the following sub-categories:

Category 1: Known human genes (from the literature or public databases). *Subcategory 1.1*: Genes with 100% identity over a complete cDNA with defined functional association (for example, transcription factor, kinase). *Subcategory 1.2*: Genes with 100% identity over a complete cDNA corresponding to a gene of unknown function (for example, some of the KIAA series of large cDNAs).

Category 2: Novel genes with similarities over essentially their total length to a cDNA or open reading frame (ORF) of any organism. *Subcategory 2.1*: Genes showing similarity or homology to a characterized cDNA from any organism (25–100% amino-acid identity). This class defines new members of human gene families, as well as new human homologues or orthologues of genes from yeast, *Caenorhabditis elegans*, *Drosophila*, mouse and so on. *Subcategory 2.2*: Genes with similarity to a putative ORF predicted *in silico* from the genomic sequence of any organism but which currently lacks experimental verification.

Category 3: Novel genes with regional similarities to confined protein regions. *Subcategory 3.1*: Genes with amino-acid similarity confined to a protein region specifying a functional domain (for example, zinc fingers, immunoglobulin domains). *Subcategory 3.2*: Genes with amino-acid similarity confined to regions of a known protein without known functional association.

Category 4: Novel anonymous genes defined solely by gene prediction. These are putative genes lacking any detectable similarity to known proteins or protein motifs. These models are based solely on spliced EST matches, consistent exon prediction or both. *Subcategory 4.1*: Predicted genes composed of a pattern of two or more consistent exons (located within <20 kb) and supported by spliced EST match(es). *Subcategory 4.2*: Predicted genes corresponding to spliced EST(s) but which failed to be recognized by exon prediction programs. *Subcategory 4.3*: Predicted genes composed only of a pattern of consistent exons without any matches to ETS(s) or cDNA. Intuitively, predicted genes from subcategory 4.1 are considered to have stronger coding potential than those of subcategory 4.3.

Category 5: Pseudogenes may be regarded as gene-derived DNA sequences that are no longer capable of being expressed as protein products. They were defined as predicted polypeptides with strong similarity to a known gene, but showing at least one of the following features: lack of introns when the source gene is known to have an intron/exon structure, occurence of in-frame stop codons, insertions and/or deletions that disrupt the ORF or truncated matches. Generally, this was an unambiguous classification.

When a gene could fulfil more than one of these criteria, it was placed into the higher possible category (for example, gene prediction with spliced EST exhibiting a significant match to a known protein was placed in subcategory 2.2 rather than 4.2).

The gene content of chromosome 21. For the gene catalogue of chromosome 21, see Table 2. The chromosome contains 225 genes and 59 pseudogenes. Of these, 127 correspond to known genes (subcategories 1.1 and 1.2) and 98 represent putative novel genes predicted *in silico* (categories 2, 3 and 4). Of the novel genes, 13 are similar to known proteins (subcategories 2.1 and 2.2), 17 are anonymous ORFs featuring modular domains (subcategories 3.1 and 3.2), and most (68 genes) are anonymous transcription units with no similarity to known proteins (subcategories 4.1, 4.2 and 4.3). Our data show that about 41% of the genes that were identified on chromosome 21 have no functional attributes.

In a rough generic description, the gene catalogue of chromosome 21 contains at least 10 kinases (PRED1, PRSS7, C21orf7, PRED33, PRKCBP2, DYRKA1, ANKDR3, SNF1LK, PDXK and PFKL), five genes involved in ubiquitination pathways (USP25, USP16, UBASH, UBE2G2 and SMT3H1), five cell adhesion molecules (NCAM2, IGSF5, C21orf43, DSCAM and ITGB2), a number of transcription factors and seven ion channels (C21orf34, KCNE2, KCNE1, CILC1L, KCNJ6, KCNJ15 and TRPC7). Several clusters of functionally related genes are arranged in tandem arrays on 21q, indicating the likelihood of ancient sequential rounds of gene duplication. These clusters include the five members of the interferon receptor family that spans 250 kb on 21q (positions 20,179,027–20,428,899), the trefoil peptide cluster (TFF1, TFF2 and TFF3) spanning 54 kb on 21q22.3 (positions 29,279,519–29,333,970) and the keratin-associated protein (KAP) cluster spanning 164 kb on 21q22.3 (positions 31,468,577–31,632,094) (Table 2). The last contains 18 units of this highly repetitive gene family featuring genes and different pseudogene fragments and revealing inverted duplications within the gene cluster (described below). Finally, the p arm of chromosome 21 contains at least one gene (TPTE) encoding a putative tyrosine phosphatase. This is the first description of a protein-coding gene mapping to the p arm of an acrocentric chromosome. However, the functional activity of this gene remains to be demonstrated.

Chromosome 21 contains a very low number of identified genes (225) compared with the 545 genes reported for chromosome 22 (ref. 10). Figure 1 shows the overall distribution of the 225 genes and 59 pseudogenes on chromosome 21 in relation to compositional features such as G+C content, CpG islands, Alu and L1 repeats and the positions of selected STSs, polymorphic markers and chromosomal breakpoints. Earlier reports indicated that gene-rich regions are Alu rich and LINE1 poor, whereas gene-poor regions contain

Table 2 Gene catalogue of chromosome 21. The table displays the gene symbol, accession number, gene description, gene category, orientation, gene start position, gene end position, genomic size and corresponding genomic clone name. The gene categories are colour coded as follows: known genes (category 1) in red, novel genes with similarities to characterized cDNAs from any organism and novel genes with similarities to protein domains (categories 2 and 3) in green, novel gene prediction (category 4) in blue, and pseudogenes (category 5) in purple. Coordinates are given in base pairs.

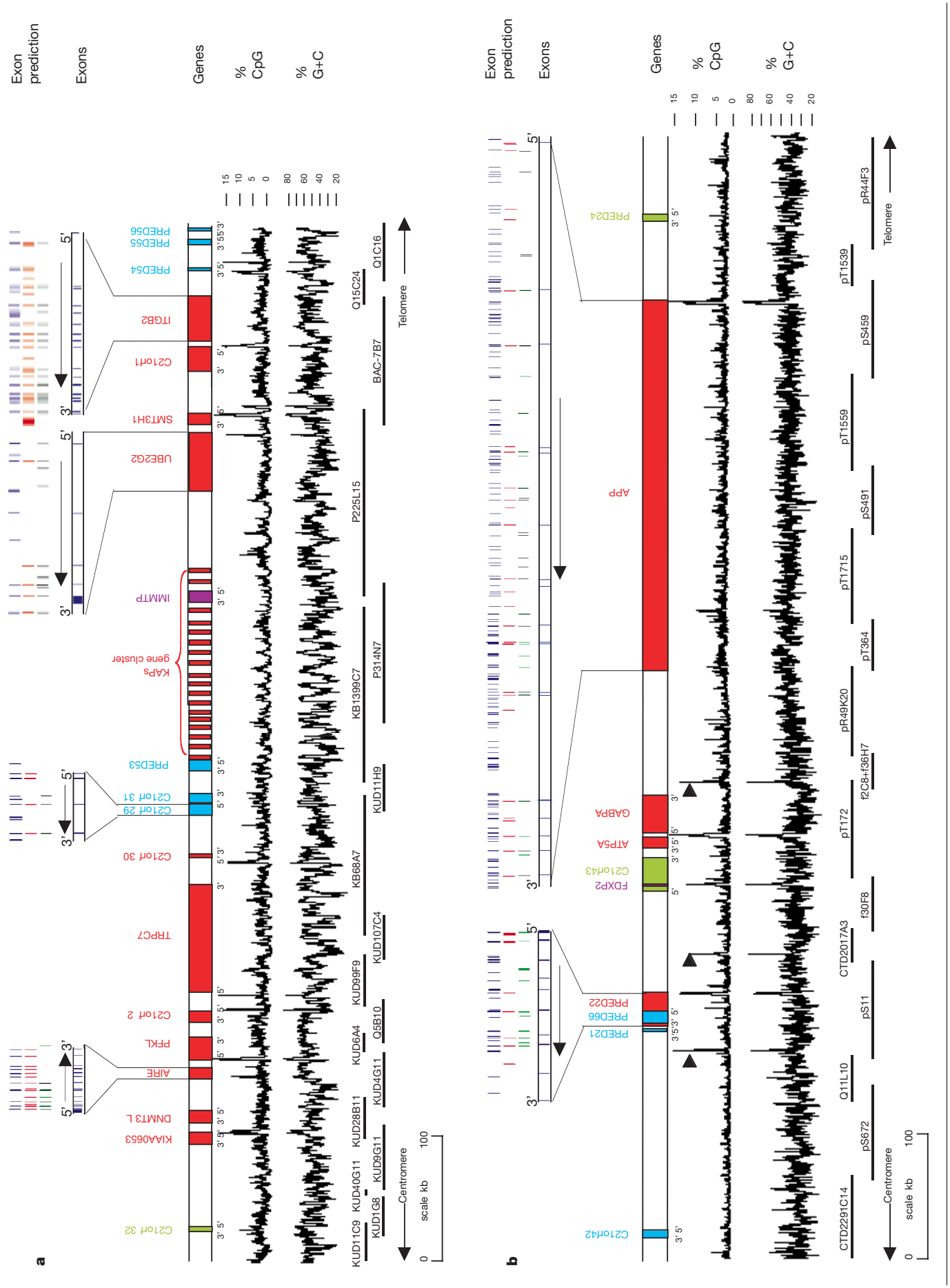

more LINE1 elements at the expense of Alu sequences[11]. Our data, and the comparison with chromosome 22, support these findings (see Tables 1 and 2, Fig. 1 and ref. 10). There is a large 7-Mb region (between 5 and 12 Mb on Fig. 1) with low G+C content (35% compared with 43% for the rest of the chromosome) that correlates with a paucity of both Alu sequences and genes. Only two known genes (PRSS7 and NCAM2) and five predicted genes can be found in this region. Further reinforcing the concept that compositional features correlate with gene density, Fig. 2 compares the genomic organization and gene density in a 831-kb G+C-rich DNA region (53%; Fig. 2a) with that of a 915-kb DNA stretch representative of a G+C-poor region (39.5%; Fig. 2b). Figure 2a shows eleven known genes, seven predicted genes, one pseudogene and the KAP cluster. Figure 2b shows four known genes, five predicted genes and one pseudogene. Figure 2 also displays examples of exon/intron structures as defined by the exon prediction programs in parallel with the real gene structure that was obtained by sequence alignment using the cognate mRNA. Most exons were predicted by the combination of the three programs. However, MZEF tends to overpredict exons compared with GRAIL and GENSCAN, in particular for the large APP gene. In addition, CpG islands correlate well as indicators of the 5′ end of genes in both of these regions.

Structural features of known and predicted genes. Among the 127 known genes, 22 genes are larger than 100 kb, the largest being DSCAM (840 kb). Seven of the largest known genes cover 1.95 Mb and lie within a region of 4.5 Mb (positions 23.7 Mb–28.2 Mb) that contains only four predicted genes and two pseudogenes. The average size of the genes is 39 kb, but there is a bias in favour of the category 1 genes. Known genes have a mean size of 57 kb, whereas predicted genes (categories 2, 3 and 4) have a mean size of 27 kb. This is not unexpected, because of the inherent difficulties in extending exon prediction to full-length gene identification. For instance, exon prediction and EST findings are usually not exhaustive. This would also explain the fact that 69% of the predicted genes have no similarity to known proteins.

Despite the shortcomings of current gene prediction methods, all known genes previously shown to map on chromosome 21 (ref. 12) were identified independently by *in silico* methods. Patterns of consistent exon prediction alone were sufficient to locate at least partial gene structures for more than 95% of these. This was true even for large A+T-rich genes, such as NCAM2, APP (Fig. 2b) and GRIK1. These three genes are several hundred kilobases long with a G+C content of 38–40%, but most exons were well predicted and enough introns were sufficiently small that a clear pattern of consistent exons was seen. In addition, more than 95% of the known genes were independently identified from spliced ESTs. Characteristics of genes that could be missed using our detection methods include those with poor exon prediction and long 3′ untranslated regions (>2 kb); those with poor exon prediction and very restricted expression pattern; and those with very large introns (>30 kb).

We designed our gene identification criteria to extract most of the coding potential of the chromosome and to minimize false positive predictions. Errors to be expected in the predictions include false positive exons, incorrect splice sites, false negative exons, fusion of multiple genes into one transcription unit and separation of a single gene into two or more transcription units. We believe that our method is sufficiently robust to pinpoint real genes, but our models still require experimental validation. In a pilot experiment on 14 predicted category 4 genes we performed RT-PCR (PCR with reverse transcription) in 12 tissues. We could confirm 11 genes and connect two gene predictions into a single transcription unit.

Pseudogenes are often overlooked in a gene catalogue aimed at specifying functional proteins, but they may be important in influencing recombination events. The 59 pseudogenes described here are not randomly located in the chromosome (Fig. 1). Twenty-four pseudogenes are distributed in the first 12 Mb of 21q, which is a gene-poor region. In contrast, a cluster of 11 pseudogenes was found within a 1-Mb stretch of DNA that is gene rich and corresponds precisely to the highest density of Alu sequences on the chromosome (positions 22,421,026–23,434,597).

Base composition and gene density. It is tempting to speculate on possible correlations between the base composition, gene density and molecular architecture of the chromosome bands. Giemsa-dark chromosomal bands are comprised of L isochores (<43% G+C), whereas Giemsa-light bands have variable composition. The latter include L, H1/H2 (43–48% G+C) and H3 isochores (>48% G+C)[13]. In humans, the average gene density is around one gene per 150 kb in L, one per 54 kb in H1/H2 and one per 9 kb in H3 isochores[14]. The proximal half of 21q (from 0.2 to 17.7 Mb of Fig. 1), which corresponds mainly to the large Giemsa dark band, 21q21, comprises a long continuous L isochore, harbouring extensive stretches of 34–37% G+C, and rare segments of more than 40% G+C. Twenty-five category 1 genes and 33 category 2–4 genes were found in this region, giving an average density of one gene per 301 kb.

The distal half of 21q (17.7–33.5 Mb) largely comprises stretches of H1/H2 isochores alternating with L isochores, and H3 isochores localized within the region spanning positions 29–33.5 Mb. The overall gene density in the telomeric half is much higher than that in the proximal half: 101 genes of category 1 and 66 genes of categories 2–4 were found in this region, giving an average of about one gene per 95 kb. The DSCAM gene, found within an L isochore in this region, spans 834 kb. In contrast, the region spanning the H3 isochores contains 46 category 1 genes and 31 category 2–4 genes, averaging one gene per 58 kb.

The L isochores have lower gene density than that predicted from whole-genome analysis: one gene per 301 kb compared with one per 150 kb. The H3 isochores are also lower in gene content, averaging one gene per 58 kb compared with one gene per 9 kb estimated for the genome as a whole. This discrepancy may be due to an overestimation of the total number of human genes based on EST data (see below). Alternatively, we may have missed half of the genes on this chromosome. This second possibility is unlikely as more than 95% of the known genes have been predicted using our criteria.

Chromosomal structural features

Duplications within chromosome 21. The unmasked sequence of the whole chromosome was compared with itself to detect intra-chromosomal duplications. We identified a 10-kb duplication in the pericentromeric regions of the p- and q-arms (Fig. 3a). The p-arm copy extends from 190 to 199 kb of the p-arm contig, and the q-arm copy extends from 405 to 413 kb of the 21q sequence. We identified a CpG island on the centromeric side of the duplication in the p-arm, indicating that there may be an active gene in the vicinity of the duplicated regions. A similar structure was reported for chromosome 10 (ref. 15), so such repeats close to the centromere may have a functional role. The pericentromeric region in the q-arm also contains several duplications, including several clusters of α-satellite sequences and even telomeric satellites

Another duplication corresponding to a large 200-kb region has been identified in proximal and distal locations on 21q (Fig. 3b). This duplication was previously reported[16] but was not analysed in detail at the sequence level. The proximal copy is located from 188 to 377 kb in 21q11.2, whereas the distal copy lies in 21q22 and extends from 14,795 to 15,002 kb. The two copies are highly conserved and

Figure 2 Gene organization on chromosome 21. **a**, A G+C-rich region of the telomeric part; **b**, an AT-rich region of the centromeric part. Genes are represented by coloured boxes. Category 1, red; categories 2 and 3, green; category 4, blue; category 5, violet. Predicted exons shown in the enlarged gene areas are represented as: MZEF, blue; Genscan, red; Grail, green. Arrowheads, orphan CpG islands that may indicate the presence of a cryptic gene.

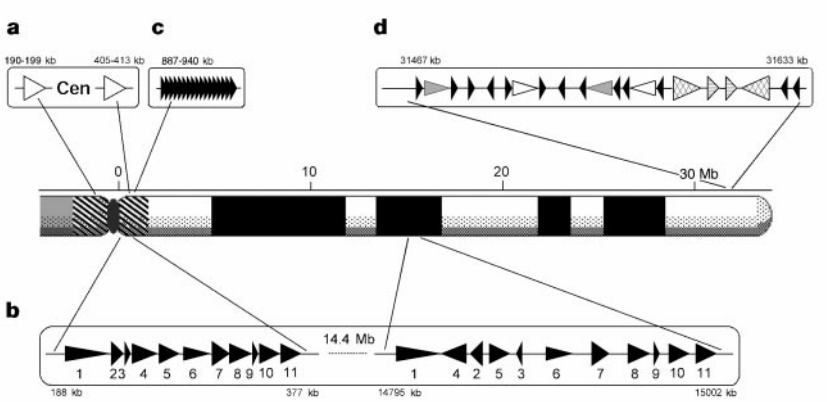

Figure 3 Schematic view of the duplicated regions in chromosome 21 as described in the text. **a**–**d**, Duplicated regions. The positions of each repeat structure are shown in kb starting at the centromere. The arrowheads represent the orientation and approximate size of each repetitive unit.

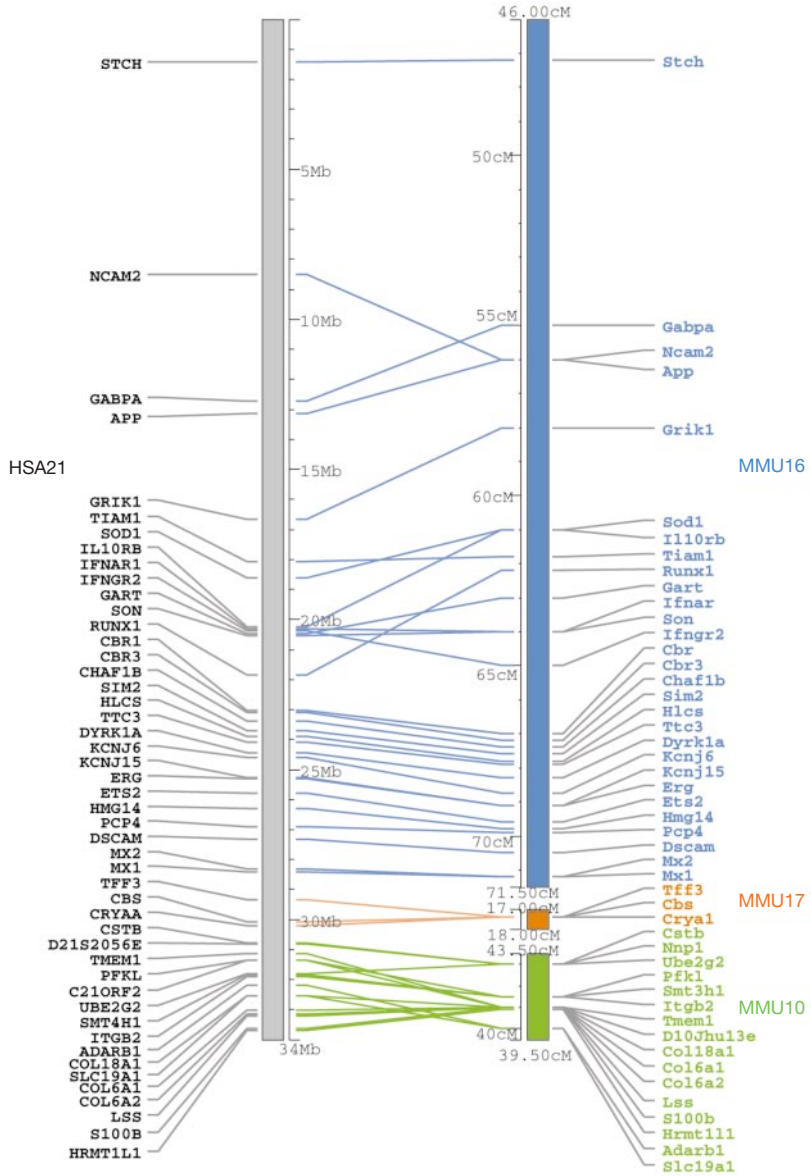

Figure 4 Schematic view of the syntenic regions between human chromosome 21 (HSA21) and mouse chromosomes 16 (MMU16), 17 (MMU17) and 10 (MMU10). Left: sequence map of human chromosome 21. Right: corresponding mouse chromosomes. Each pair of syntenic markers is joined with a line.

show 96% identity. We detected two large inversions, several other rearrangements and several translocations or duplications within the duplicated units (Fig. 3b), which caused segmentation of the units into at least 11 pieces. The distal copy is 207 kb long and the proximal copy is 189 kb; the 18-kb size difference between the two duplicated segments is due to insertions in the distal copy, deletions in the proximal copy or both.

In the region on 21q between 887 and 940 kb a block of sequence is repeated 17 times (Fig. 3c). The similarity of these repetitive units indicates that they were formed by a recent triplication event of a region of six repeat unit blocks, which had in turn been generated by duplication of a three-block unit.

Another repeat sequence lies between the TRPC7 and UBE2G2 genes on 21q22.3 (31,467–31,633 kb). This feature corresponds to the 166-kb KAP gene and pseudogene cluster described above (Fig. 2a). A 0.5–1-kb segment is repeated at least 13 times, with 5–10-kb spacer intervals (Fig. 3d). The repeat units share more than 91% identity with each other.

Comparison of chromosome 21 with chromosome 22. The two chromosomes are similar in size, and both are acrocentric. The gene density, however, is much higher on chromosome 22 (ref. 10). We detected sequence similarity in the pericentromeric and sub-telomeric regions of both chromosomes. For example, two different regions in the 21p contig (42–84 kb; 239–263 kb) are duplicated in 22q (1043–1067 kb; 1539–1564 kb). These duplications are located within the pericentromeric regions of both chromosomes[17]. Half of the first region is further duplicated at the position 22,223–22,248 kb in chromosome 22. In addition, two inverted duplications in 21q at 88–156 kb and 646–751 kb have also been observed on 22q at positions 572–637 kb and 45–230 kb. Large clusters of α-satellite sequences (10 kb for chromosome 21 and 119 kb for chromosome 22) are located on 21q (88–156 kb) and 22q (572–637 kb).

The most telomeric clone, F50F5, isolated from the chromosome-specific CMF21 fosmid library, contains a telomeric repeat array that represents the hallmark of the telomeric end of a chromosome. This array was missing in the chromosome 22q sequence[10]. However, the 22q sequence ends very near to the telomere, considering that it shows strong homology with a 2.5–10-kb stretch of telomeric sequence present in F50F5.

Comparison of chromosome 21 with other autosomes. In the most telomeric region of chromosome 21 we also identified a novel repeat structure featuring a non-identical 93-bp unit that is repeated 10 times. This block of 93-bp repeats is located 7.5 kb from the start point of the telomeric array. Similar 93-bp repeat sequences were also detected by BLAST analysis in chromosomes 22, 10 and 19. FISH analysis data suggest that this 93-bp repeat unit is also located on 5qter, 7pter, 17qter, 19pter, 19qter, 20pter, 21qter and 22qter, as well as on other chromosomal ends. Thus, this 93-bp repeat may be a common structural feature shared by many human telomeres.

We have found some paralogous regions between chromosome 21 and other human chromosomes, which were also pointed out by metaphase FISH analysis of the corresponding genomic clones. For example, a 100-kb region of clone B15L0C0 located on 21p is shared with chromosomes 4, 7, 20 and 22. A second homologous region of 50 kb on 21q between 15,530 and 15,580 kb is shared with a segment on chromosome 16 between the genes 44M2.1 and 44M2.2. More details on these regions can be found at http://hgp.gsc.riken.go.jp/.

Synteny with mouse. Human chromosome 21 shows conserved syntenies to mouse chromosomes 16, 17 and 10 (http://www.informatics.jax.org/). Figure 4 shows a comparative map of human chromosome-21-specific genes with their mouse orthologues. A number of inversions can be seen. These changes in gene order may be due to rearrangements during genome evolution. Alternatively, they may reflect the fact that the mouse gene map is still inaccurate because it is based on linkage and physical mapping.

Breakpoints. Figure 1 shows the locations of 39 breakpoints on the physical map. Here we describe several classes of breakpoint, all of which either occurred naturally in the human population before hybrid construction or were induced by irradiation. The natural breakpoints arose mainly from reciprocal translocations of chromosome 21 with other human chromosomes (6;21, 4;21, 3;21, 1;21, 8;21, 10;21, 11;21 and 21;22). A second class of naturally occurring breakpoints derived from intrachromosomal rearrangements of chromosome 21 (ACEM, 6918, MRC2, R210 and DEL21). A third class of breakpoints, designated 3x1, 3x2, 1x4D, 1x4F and 1x18, were generated experimentally by irradiation of hybrids containing intact chromosome 21q arms[18]. Hybrids 2Fur, 750 and 511 represent rearrangements of chromosome 21 that occurred spontaneously in somatic cell hybrids. All of these chromosome derivatives were isolated in Chinese hamster ovary (CHO) × human somatic cell hybrids.

Fine mapping revealed an uneven distribution of breakpoints that fell roughly in two clusters on chromosome 21. Nine breakpoints occur within the pericentromeric region (0–2.2 Mb) and another nine are located within a 2.4-Mb region in 21q22 (20.1–22.5 Mb) (Fig. 1). In contrast, large regions are totally devoid of breakpoints. For instance, only two translocation breakpoints are located in the 10-Mb region between 4.95 and 14.4 Mb of the q arm.

Several breakpoints occur within or near the duplicated regions described above. For instance, three breakpoints (1x4D, 1x18 and 2Fur) occur between positions 100 and 400 kb on 21q. This region corresponds to the proximal copy of the large duplicated region described in Fig. 3b. Another breakpoint (ACEM) occurs between positions 14,400 and 14,525 kb, close to the distal copy of this duplicated region. We also found a naturally occurring 21;22 translocation breakpoint (position 31,350–31,380 kb) in the KAP cluster.

Duplicated regions may mediate certain mechanisms involved in chromosomal rearrangement. It is likely that similar sequence features may be important for duplication, genetic recombination and chromosomal rearrangement. Further sequence analysis will help to unravel the underlying molecular mechanisms of chromosome breakage and recombination.

Recombination. The distribution of the recombination frequency on chromosome 21 is different in males and females[12]. In Fig. 5 genetic distances of known polymorphic markers from male, female and sex-average maps are compared with the distances in nucleotides on 21q. The recombination frequency is relatively higher near the centromere in females and near the telomere in males. This confirms earlier analysis based on physical maps[11]. Unlike chromosome 22, chromosome 21 does not appear to contain particular regions with a steep increase in recombination frequency in the middle of the chromosome.

Medical implications

Down syndrome. Besides the constant feature of mental retardation, individuals with Down syndrome also frequently exhibit congenital heart disease, developmental abnormalities, dysmorphic features, early-onset Alzheimer's disease, increased risk for specific leukaemias, immunological deficiencies and other health problems[19]. Ultimately, all these phenotypes are the result of the presence of three copies of genes on chromosome 21 instead of two. Data from transgenic mice indicate that only a subset of the genes on chromosome 21 may be involved in the phenotypes of Down syndrome[20]. Although it is difficult to select candidate genes for these phenotypes, some gene products may be more sensitive to gene dosage imbalance than others. These may include morphogens, cell adhesion molecules, components of multi-subunit proteins, ligands and their receptors, transcription regulators and transporters. The gene catalogue now allows the hypothesis-driven selection of different sets of candidates, which can then be used to study the molecular pathophysiology of the gene dosage effects. The complete catalogue will also provide the opportunity to

search systematically for candidate genes without pre-existing hypotheses.

Monogenic disorders. Mutations in 14 known genes on chromosome 21 have been identified as the causes of monogenic disorders including one form of Alzheimer's disease (APP), amyotrophic lateral sclerosis (SOD1), autoimmune polyglandular disease (AIRE), homocystinuria (CBS) and progressive myoclonus epilepsy (CSTB); in addition, a locus for predisposition to leukaemia (AML1) has been mapped to 21q (for details of each of these disorders, see http://www.ncbi.nlm.nih.gov/omim/). The cloning of some of these genes, including the AIRE gene[21,22], was facilitated by the sequencing effort. Loci for the following monogenic disorders have not yet been cloned: recessive nonsyndromic deafness (DFNB10 (ref. 23) and DFNB8 (ref. 24)), Usher syndrome type 1E[25], Knobloch syndrome[26] and holoprocencephaly type 1 (HPE1 (ref. 27)). The gene catalogue and mapping coordinates will help in their identification. Mutation analysis of candidate genes in patients will lead to the cloning of the responsible genes.

Complex phenotypes. Two loci conferring susceptibility to complex diseases have been mapped to chromosome 21 (one for bipolar affective disorder[28] and one for familial combined hyperlipidaemia[29]) but the genes involved remain elusive.

Neoplasias. Loss of heterozygosity has been observed for specific regions of chromosome 21 in several solid tumours[30–36] including cancers of the head and neck, breast, pancreas, mouth, stomach, oesophagus and lung. The observed loss of heterozygosity indicates that there may be at least one tumour suppressor gene on this chromosome. The decreased incidence of solid tumours in individuals with Down syndrome indicates that increased dosage of some chromosome 21 genes may protect such individuals from these tumours[37–39]. On the other hand, Down syndrome patients have a markedly increased risk of childhood leukaemia[19], and trisomy of chromosome 21 in blast cells is one of the most common chromosomal aneuploidies seen in childhood leukaemias[40].

Chromosome abnormalities. Chromosome 21 is also involved in chromosomal aberrations including monosomies, translocations and other rearrangements. The availability of the mapped and sequenced clones now provides the necessary reagents for the accurate diagnosis and molecular characterization of constitutional and somatic chromosomal abnormalities associated with various phenotypes. This, in turn, will aid in identifying genes involved in mechanisms of disease development.

The analysis of the genetic variation of many of the genes on chromosome 21 is of particular importance in the search for associations of polymorphisms with complex diseases and traits. Single nucleotide polymorphism (SNP) genotyping may also aid in the identification of modifier genes for numerous pathologies. Similarly, SNPs are useful tools in the development of diagnostic and predictive tests, which may eventually lead to individualized treatments. Chromosome-21-specific nucleotide polymorphisms will also facilitate evolutionary studies.

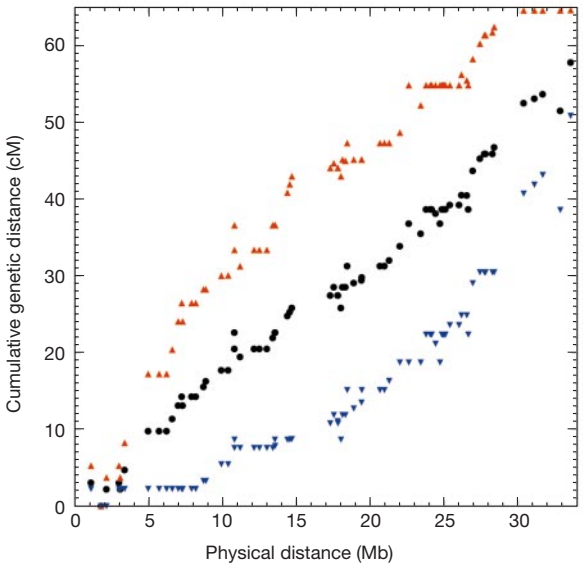

Figure 5 Comparison of the genetic map and the sequence map of chromosome 21 aligned from centromere to telomere. Genetic distance in cM; physical distance in Mb. Each spot reflects the position of a particular genetic marker retrieved from http://www.marshmed.org. Black circles, sex-average; orange upwards triangles, female; blue downwards triangles, male.

Discussion

Our sequencing effort provided evidence for 225 genes embedded within the 33.8 Mb of genomic DNA of chromosome 21. Five hundred and forty-five genes have been identified in the 33.4 Mb of chromosome 22 (ref. 10). These data support the conclusion that chromosome 22 is gene-rich, whereas chromosome 21 is gene-poor. This finding is in agreement with data from the mapping of 30,181 randomly selected Unigene ESTs[41]. These two chromosomes together represent about 2% of the human genome and collectively contain 770 genes. Assuming that both chromosomes combined reflect an average gene content of the genome, we estimate that the total number of human genes may be close to 40,000. This figure is considerably lower than previous estimates, which range from 70,000 to 140,000 (ref. 42), and which were mainly based on EST clustering. It is possible that not all of the genes on chromosomes 21 and 22 have been identified. Alternatively, our assumption that the two chromosomes represent good models may be incorrect.

Our analysis of the chromosomal architecture revealed repeat units, duplications and breakpoints. A 93-bp repeat in the telomeric region, which was also found in other chromosomes, should provide a basis for studying the structural and functional organization and evolution of the telomere. One striking feature of chromosome 21 is that there is a 7-Mb region (positions 5.5–12.5 Mb) that contains only one gene. This region is much larger than the whole genome of *Escherichia coli*, but the evolutionary process permitted the existence of such a gene-poor DNA segment. Three other 1-Mb regions on 21q are also devoid of genes. Together, these gene-poor regions comprise almost 10 Mb, which is one-third of chromosome 21. Chromosome 22 also has a 2.5-Mb region near the telomeric end, as well as two other regions, each of 1 Mb, which are devoid of genes. We propose that similar large gene-less or gene-poor regions exist in other mammalian chromosomes. These regions may have a functional or architectural significance that has yet to be discovered.

Having the complete contiguous sequence of human chromosomes will change the methodology for finding disease-related genes. Disease genes will be identified by combining genetic mapping with mutation analysis in positional candidate genes. The laborious intermediate steps of physical mapping and sequencing are no longer necessary. Therefore, any individual investigator will be able to participate in disease gene identification.

The complete sequence analysis of human chromosome 21 will have profound implications for understanding the pathogenesis of diseases and the development of new therapeutic approaches. The clone collection represents a useful resource for the development of new diagnostic tests. The challenge now is to unravel the function of all the genes on chromosome 21. RNA expression profiling with all chromosome-21-specific genes may allow the identification of up- and downregulated genes in normal and disease samples. This approach will be particularly important for studying expression differences in trisomy and monosomy 21. Furthermore, chromosome-21-homologous genes can be systematically studied by overexpression and deletion in model organisms and mammalian cells.

The relatively low gene density on chromosome 21 is consistent with the observation that trisomy 21 is one of the only viable human autosomal trisomies. The chromosome 21 gene catalogue will open new avenues for deciphering the molecular bases of Down syndrome and of aneuploidies in general. □

Methods

Details of the protocols used by the five sequencing centres are available from our web sites (see below), including methods for the construction of sequence-ready maps and for sequencing large insert clones by shotgun cloning and nested deletion. Many software programs were used by the five groups for data processing, sequence analysis, gene prediction, homology searches, protein annotation and searches for motifs using pfam and SMART. Most of these programs are in the public domain. Software suites have been developed by the consortium members to allow efficient analysis. All information is available from the following web pages: RIKEN: http://hgp.gsc.riken.go.jp; Institut für Molekulare Biotechnologie, Jena: http://genome.imb-jena.de; Keio University: http://www-alis.tokyo.jst.go.jp/HGS/teamKU/team.html; GBF-Braunschweig: http://genome.gbf.de; Max-Planck-Institut für Molekulare Genetik (MPIMG), Berlin: http://chr21.rz-berlin.mpg.de.

Received 17 April; accepted 3 May 2000.

1. Lejeune, J., Gautier, M. & Turpin, R. Etude des chromosomes somatique des neufs enfants mongoliens. *CR Acad. Sci. Paris* **248,** 1721–1722 (1959).
2. McInnis, M. G. *et al.* A linkage map of human chromosome 21: 43 PCR markers at average intervals of 2.5 cM. *Genomics* **16,** 562–571 (1993).
3. Chumakov, I. *et al.* Continuum of overlapping clones spanning the entire human chromosome 21q. *Nature* **359,** 380–387 (1992).
4. Nizetic, D. *et al.* An integrated YAC-overlap and "cosmid-pocket" map of the human chromosome 21. *Hum. Mol. Genet.* **3,** 759–770 (1994).
5. Gardiner, K. *et al.* YAC analysis and minimal tiling path construction for chromosome 21q. *Somat. Cell Mol. Genet.* **21,** 399–414 (1995).
6. Korenberg, J. R. *et al.* A high-fidelity physical map of human chromosome 21q in yeast artificial chromosomes. *Genome Res.* **5,** 427–443 (1995).
7. Ichikawa, H. *et al.* A *Not*I restriction map of the entire long arm of human chromosome 21. *Nature Genet.* **4,** 361–366 (1993).
8. Hildmann, T. *et al.* A contiguous 3-Mb sequence-ready map in the S3-MX region on 21q22. 2 based on high-throughput nonisotopic library screenings. *Genome Res.* **9,** 360–372 (1999).
9. Hattori, M. *et al.* A novel method for making nested deletions and its application for sequencing of a 300 kb region of human APP locus. *Nucleic Acids Res.* **25,** 1802–1808 (1997).
10. Dunham, I. *et al.* The DNA sequence of human chromosome 22. *Nature* **402,** 489–495 (1999).
11. Korenberg J. R. & Rykowski, M. C. Human genome organization: Alu, lines, and the molecular structure of metaphase chromosome bands. *Cell* **53,** 391–400 (1988).
12. Antonarakis, S. E. 10 years of Genomics, chromosome 21, and Down syndrome. *Genomics* **51,** 1–16 (1998).
13. Saccone, S. *et al.* Correlations between isochores and chromosomal bands in the human genome. *Proc. Natl Acad. Sci. USA* **90,** 11929–11933 (1993).
14. Zoubak, S., Clay, O. & Bernardi, G. The gene distribution of the human genome. *Gene* **174,** 95–102 (1996).
15. Jackson, M. S. *et al.* Sequences flanking the centromere of human chromosome 10 are a complex patchwork of arm-specific sequences, stable duplications and unstable sequences with homologies to telomeric and other centromeric locations. *Hum. Mol. Genet.* **8,** 205–215 (1999).
16. Dutriaux, A. *et al.* Cloning and characterization of a 135- to 500-kb region of homology on the long arm of human chromosome 21. *Genomics* **22,** 472–477 (1994).
17. Ruault, M. Juxta-centromeric region of human chromosome 21 is enriched for pseudogenes and gene fragments. *Gene* **239,** 55–64 (1999).
18. Graw, S. L. *et al.* Molecular analysis and breakpoint definition of a set of human chromosome 21 somatic cell hybrids. *Somat. Cell. Mol. Genet.* **21,** 415–428 (1995).
19. Epstein, C. J. in *The Metabolic and Molecular Bases of Inherited Disease* (eds Scriver, C. R. *et al.*) 749–794 (McGraw-Hill, New York, 1995).
20. Kola, I. & Hertzog, P. J. Animal models in the study of the biological function of genes on human chromosome 21 and their role in the pathophysiology of Down syndrome. *Hum. Mol. Genet.* **6,** 1713–1727 (1997).
21. Nagamine, K. *et al.* Positional cloning of the APECED gene. *Nature Genet.* **17,** 393–398 (1997).
22. The Finnish-German APECED Consortium. An autoimmune disease, APECED, caused by mutations in a novel gene featuring two PHD-type zinc-finger domains. Autoimmune Polyendocrinopathy-Candidiasis-Ectodermal Dystrophy. *Nature Genet.* **17,** 399–403 (1997).
23. Bonné-Tamir, B. *et al.* Linkage of congenital recessive deafness (Gene DFNB10) to chromosome 21q22.3. *Am. J. Hum. Genet.* **58,** 1254–1259 (1996).
24. Veske, A. *et al.* Autosomal recessive non-syndromic deafness locus (DFNB8) maps on chromosome 21q22 in a large consanguineous kindred from Pakistan. *Hum. Mol. Genet.* **5,** 165–168 (1996).
25. Chaib, H. *et al.* A newly identified locus for Usher syndrome type I, USH1E, maps to chromosome 21q21. *Hum. Mol. Genet.* **6,** 27–31 (1997).
26. Sertie, A. L. *et al.* A gene which causes severe ocular alterations and occipital encephalocele (Knobloch syndrome) is mapped to 21q22.3. *Hum. Mol. Genet.* **5,** 843–847 (1996).
27. Estabrooks, L. L., Rao, K. W., Donahue, R. P., & Aylsworth, A. S. Holoprosencephaly in an infant with a minute deletion of chromosome 21(q22.3). *Am. J. Med. Genet.* **36,** 306–309 (1990).
28. Straub, R. E. *et al.* A possible vulnerability locus for bipolar affective disorder on chromosome 21q22.3. *Nature Genet.* **8,** 291–296 (1994).
29. Pajukanta, P. *et al.* Genomewide scan for familial combined hyperlipidemia genes in Finnish families, suggesting multiple susceptibility loci influencing triglyceride, cholesterol, and apolipoprotein B levels. *Am. J. Hum. Genet.* **64,** 1453–1463 (1999).
30. Sakata, K. *et al.* Commonly deleted regions on the long arm of chromosome 21 in differentiated adenocarcinoma of the stomach. *Genes Chromosome Cancer* **18,** 318–321 (1997).
31. Kohno, T. *et al.* Homozygous deletion and frequent allelic loss of the 21q11. 1–q21. 1 region including the *ANA* gene in human lung carcinoma. *Genes Chromosomes Cancer* **21,** 236–243 (1998).
32. Ohgaki, K. *et al.* Mapping of a new target region of allelic loss to a 6-cM interval at 21q21 in primary breast cancers. *Genes Chromosomes Cancer* **23,** 244–247 (1998).
33. Yamamoto, N. *et al.* Frequent allelic loss/imbalance on the long arm of chromosome 21 in oral cancer: evidence for three discrete tumor suppressor gene loci. *Oncol. Rep.* **6,** 1223–1227 (1999).
34. Ghadimi, B. M. *et al.* Specific chromosomal aberrations and amplification of the AIB1 nuclear receptor coactivator gene in pancreatic carcinomas. *Am. J. Pathol.* **154,** 525–536 (1999).
35. Bockmuhl, U. *et al.* Genomic alterations associated with malignancy in head and neck cancer. *Head Neck* **20,** 145–151 (1998).
36. Schwendel, A. *et al.* Chromosome alterations in breast carcinomas: frequent involvement of DNA losses including chromosomes 4q and 21q. *Br. J. Cancer* **78,** 806–811 (1998).
37. Satge, D. *et al.* M. A tumor profile in Down syndrome. *Am. J. Med. Genet.* **78,** 207–216 (1998).
38. Hasle, H., Clemmensen, I. H., & Mikkolsen, M. Risks of leukaemia and solid tumours in individuals with Down's syndrome. *Lancet* **355,** 165–169 (2000).
39. Satge, D. *et al.* A lack of neuroblastoma in Down syndrome: a study from 11 European countries. *Cancer Res.* **58,** 448–452 (1998).
40. Wan, T. S., Au, W. Y., Chan, J. C, Chan, L. C. & Ma, S. K. Trisomy 21 as the sole acquired karyotypic abnormality in acute myeloid leukemia and myelodysplastic syndrome. *Leuk. Res.* **23,** 1079–1083 (1999).
41. Deloukas, P. *et al.* A physical map of 30,000 human genes. *Science* **282,** 744–746 (1998).
42. Fields, C., Adams M. D., White, O. & Venter, J. C. How many genes in the human genome? *Nature Genet.* **7,** 345–346 (1994).
43. Gyapay, G. *et al.* A radiation hybrid map of the human genome. *Hum. Mol. Genet.* **5,** 339–346 (1996).
44. Stewart, E. A. *et al.* An STS-based radiation hybrid map of the human genome. *Genome Res.* **7,** 422–433 (1997).
45. Dib, C. *et al.* A comprehensive genetic map of the human genome based on 5,264 microsatellites. *Nature* **380,** 152–154 (1996).
46. Murray, J. C. *et al.* A comprehensive human linkage map with centimorgan density. *Science* **265,** 2049–2054 (1994).

Acknowledgements

The RIKEN group thank T. Itoh and C. Kawagoe for support of computational data management, M. Ohira and R. Ohki for clones and the members listed on http://hgp.gsc.riken.go.jp for technical support. The Jena group thank C. Baumgart, M. Dette, B. Drescher, G. Glöckner, S. Kluge, G. Nyakatura, M. Platzer, H.-P. Pohle, R. Schattevoi, M. Schilling, J. Weber and all present and past members of the sequencing teams. The Keio group thank E. Nakato, M. Asahina, A. Shimizu, I. Abe, J. Wang, N. Sawada, M. Tatsuyama, M. Takahashi, M. Sasaki, H. Harigai and all members of the sequencing team, past and present. The MPIMG group thank M. Klein, C. Steffens, S. Arndt, K. Heitmann, I. Langer, D. Buczek, J. O'Brien, M. Christensen, T. Hildmann, I. Szulzewsky, E. Hunt and G. Teltow for technical support, and T. Haaf and A. Palotie for help with FISH. The German groups (IMB, GBF and MPIMG) thank the Resource Center of the German Human Genome Project (RZPD) and its group members for support and for clones and resources (http://www.rzpd.de/). We also thank J. Aaltonen, J. Buard, N. Creau, J. Gröet, R. Orti, J. Korenberg, M.C. Potier and G. Roizes for bacterial clones; D. Cox for discussions; A. Fortna, H.S. Scott, D. Slavov and G. Vacano for contributions; and N. Weizenbaum for editorial assistance. The RIKEN group is mainly supported by a Special Fund for the Human Genome Sequencing Project from the Science and Technology Agency (STA) Japan, and also by a Fund for Human Genome Sequencing from the Japan Society and Technology Corporation (JST) and a Grant-in-Aid for Scientific Research from the Ministry of Education, Science, Sport and Culture, Japan. The Jena group was supported by the Federal German Ministry of Education, Research and Technology (BMBF) through Projekträger DLR, in the framework of the German Human Genome Project, and by the Ministry of Science, Research and Art of the Freestate of Thueringia (TMWFK). The Keio group was supported in part by the Fund for Human Genome Sequencing Project from the JST, Grants-in-Aid for Scientific Research, and the Fund for "Research for the Future" Program from the Japan Society for the Promotion of Science (JSPS); they also received support from Grants-in-Aid for Scientific Research on Priority Areas from the Ministry of Education, Science, Sports and Culture of Japan. The Braunschweig group was supported by BMBF through Projekträger DLR, in the framework of the German Human Genome Project. The MPIMG-Berlin group acknowledge grants from BMBF through Projekträger DLR in the framework of the German Human Genome Project and from the EU. Support also came from the Boettcher Foundation, NIH, Swiss National Science Foundation, EU and MRC.

Correspondence and requests for materials should be addressed to Y.S. (e-mail: sakaki@gsc.riken.go.jp), A.R. (e-mail: andrex1x@aol.com), N.S. (e-mail: shimizu@dmb-med.keio.ac.jp), H.B. (e-mail: bloecker@gbf.de) or M.L.Y. (e-mail: yaspo@molgen.mpg.de). Genomic clones can be requested from any of the five groups. Detailed clone information, maps, FISH data, annotated gene catalogue, gene name alias and supporting data sets are available from the RIKEN and MPIMG web sites (see Methods). Interactive chromosome 21 databases (HSA21DB) are maintained at MPIMG and RIKEN. All sequence data can be obtained from Genbank, EMBL and DDBJ. They are also available from the individual web pages.

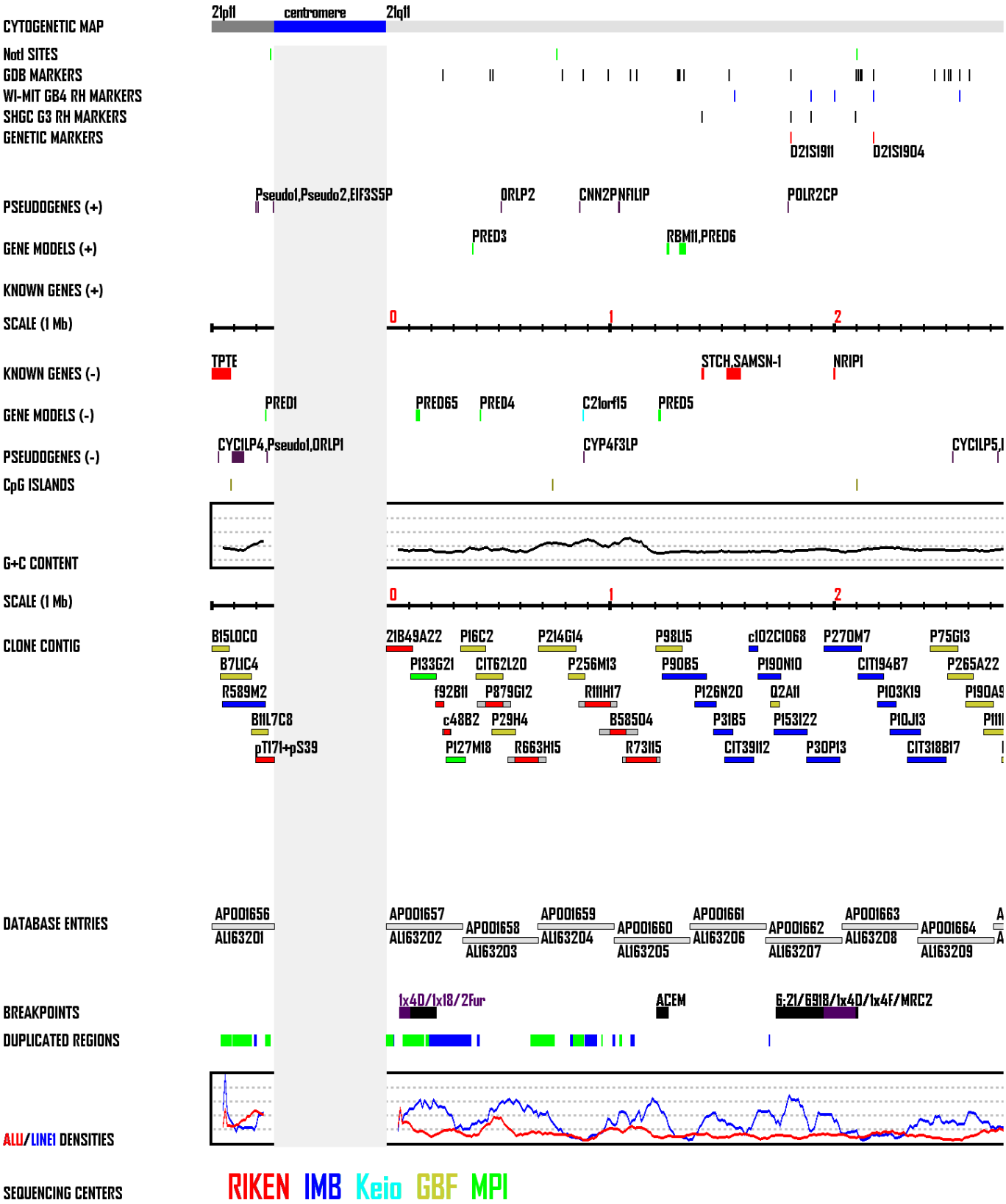

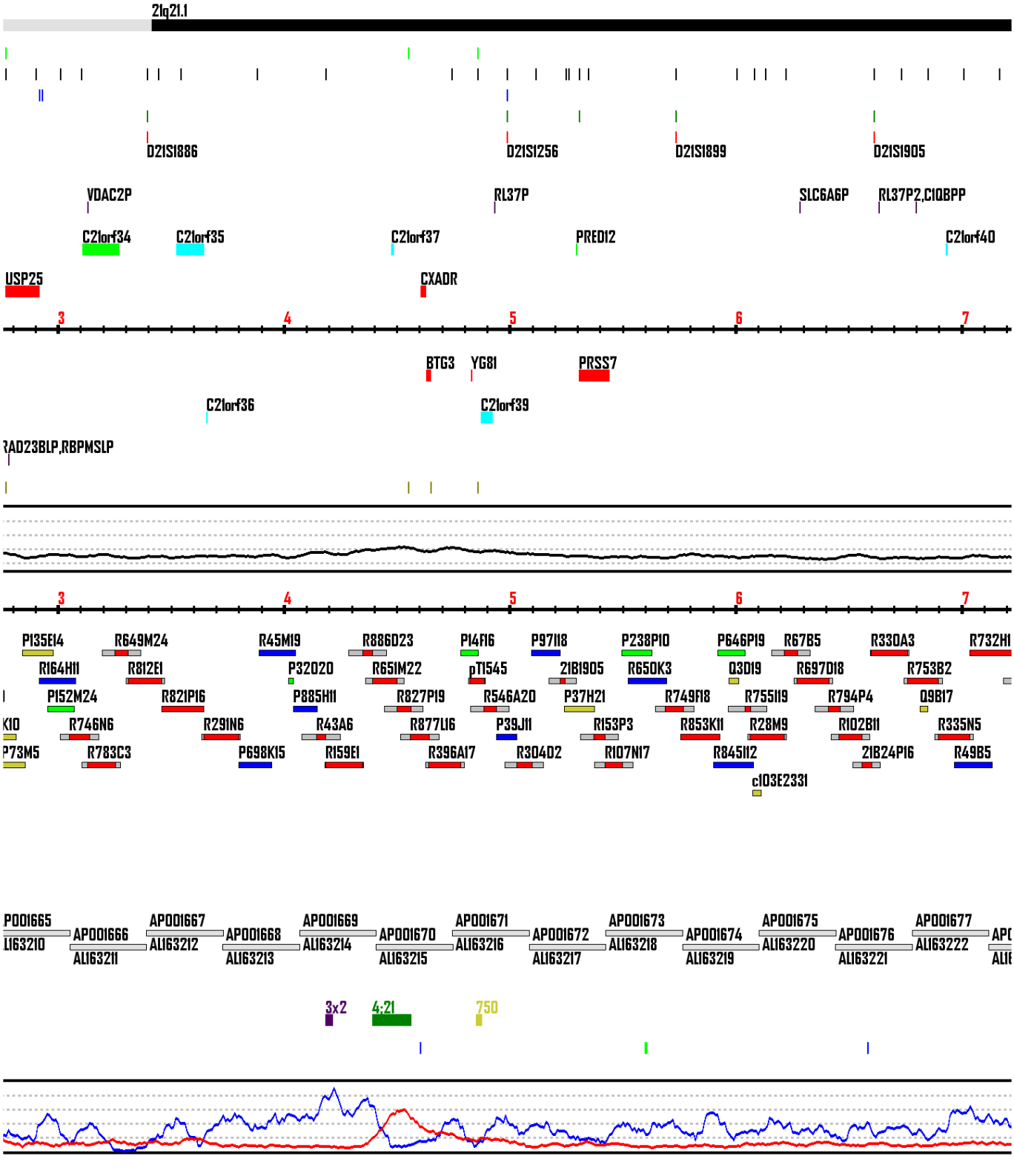

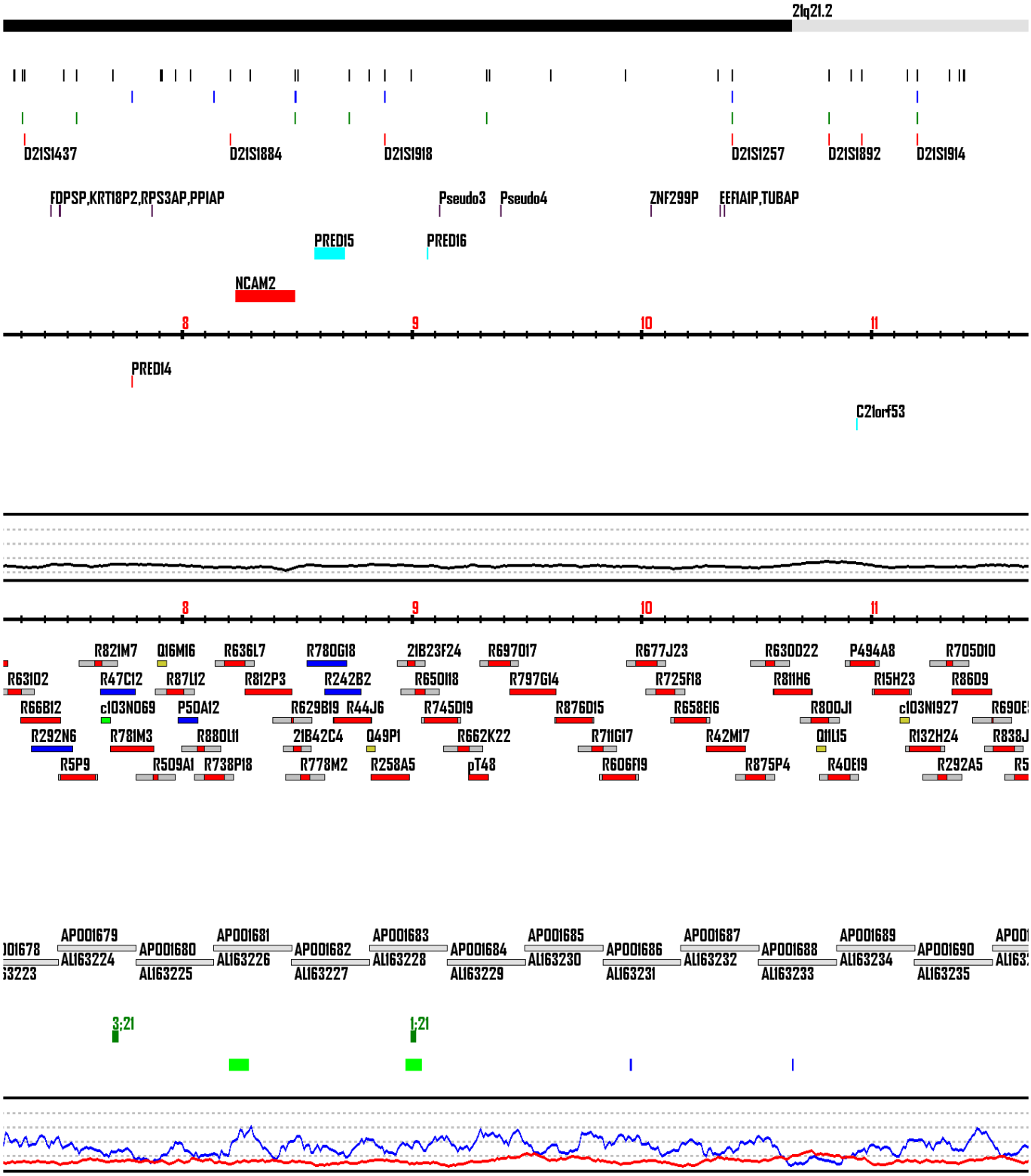

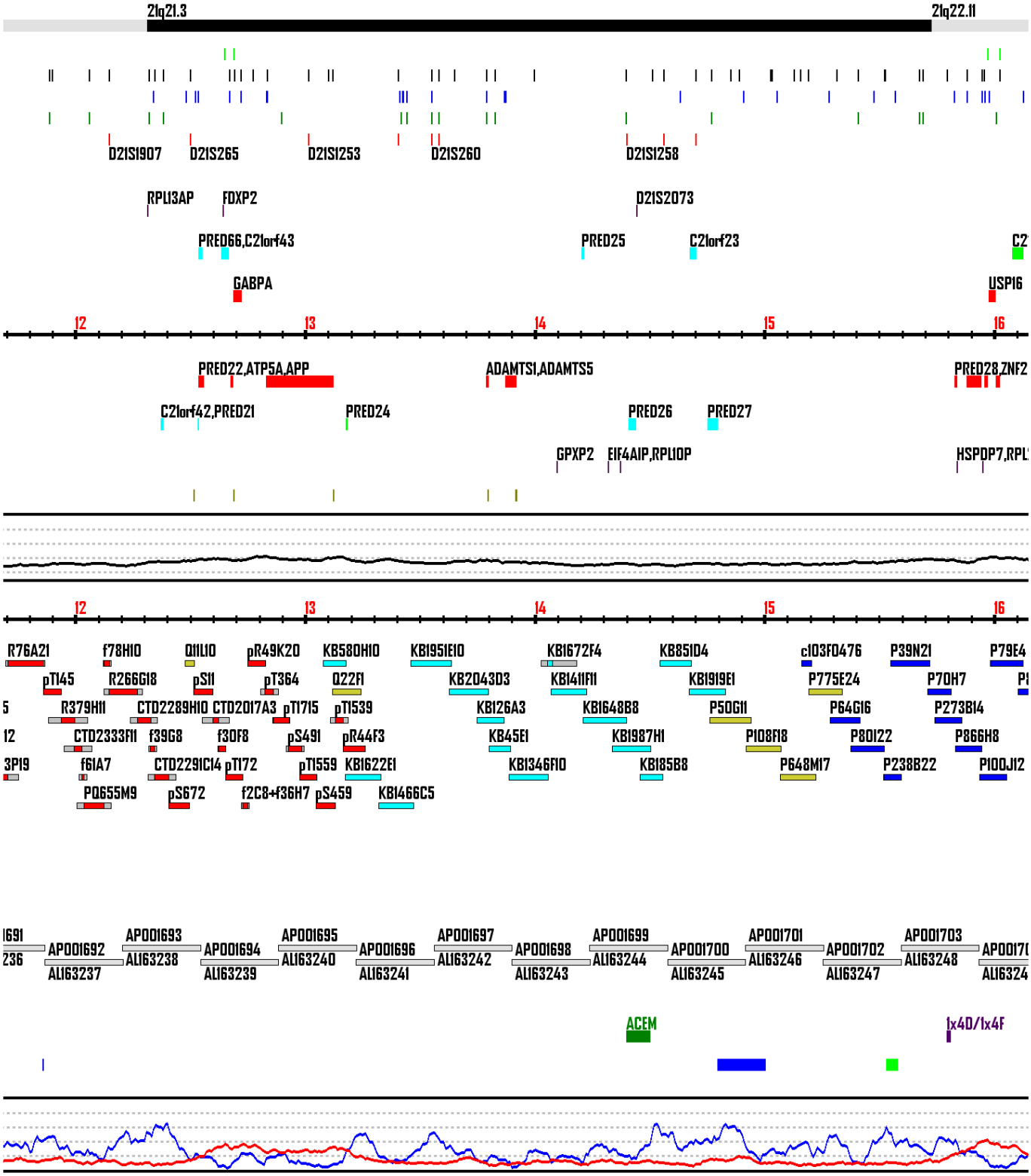

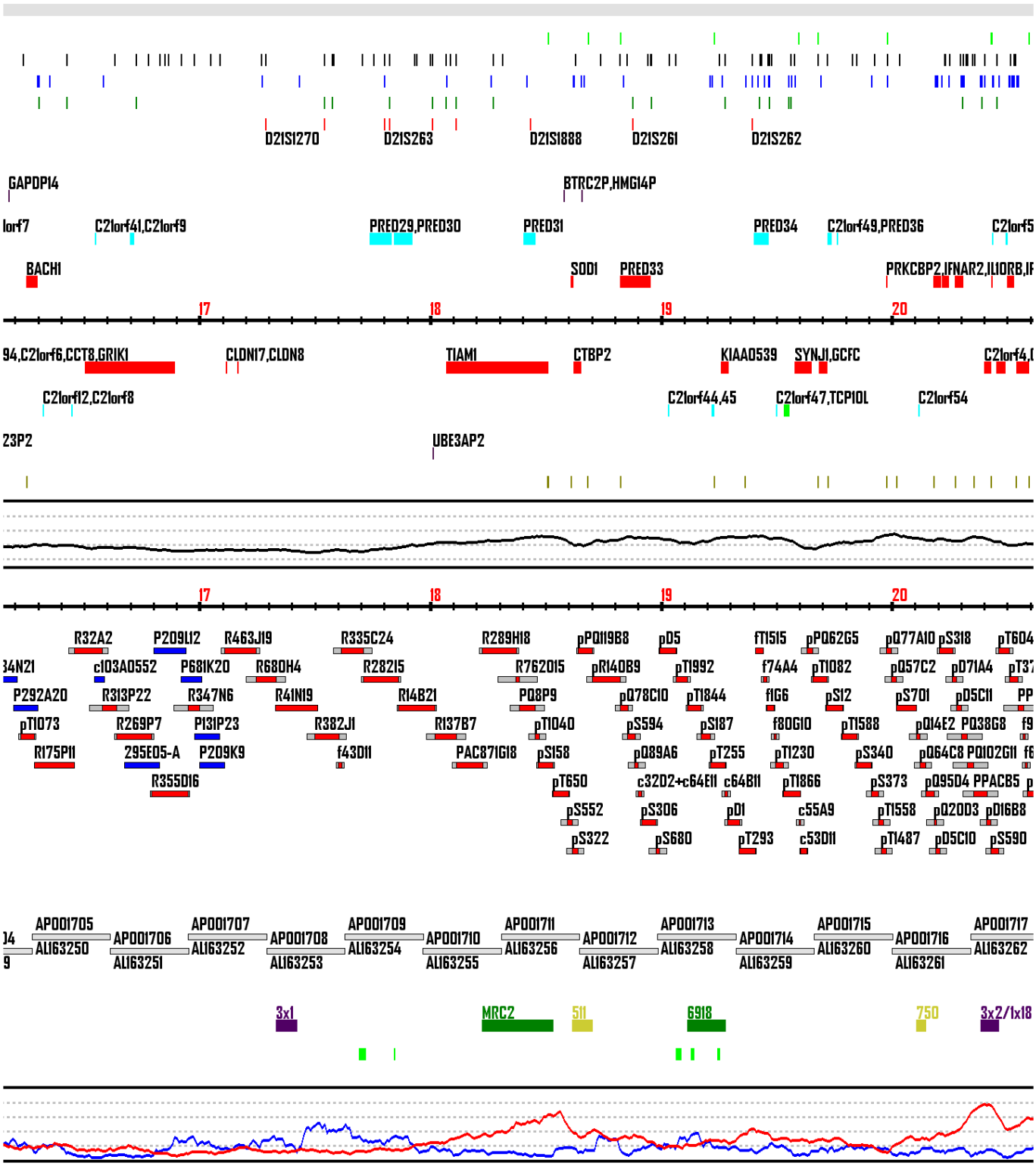

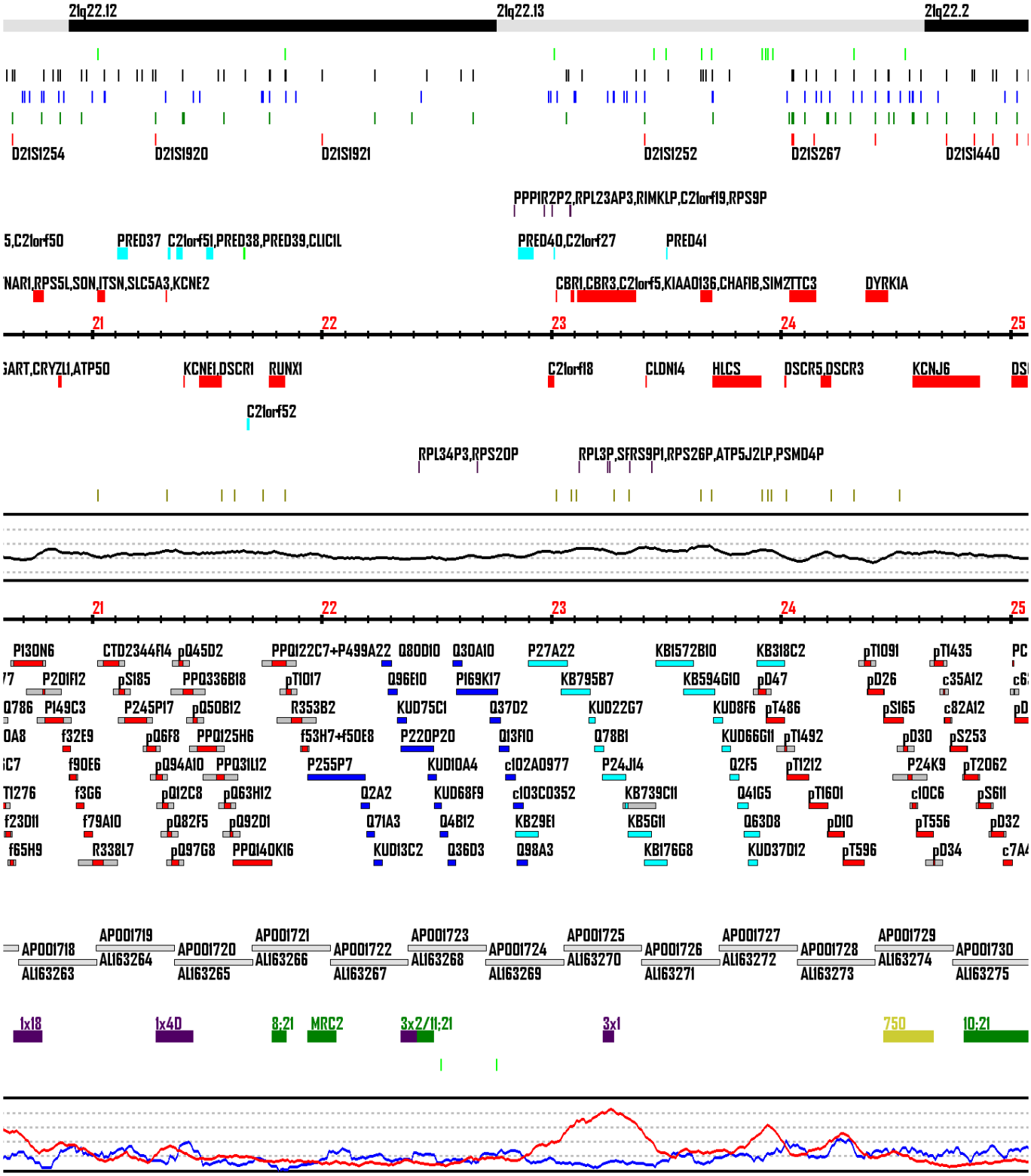

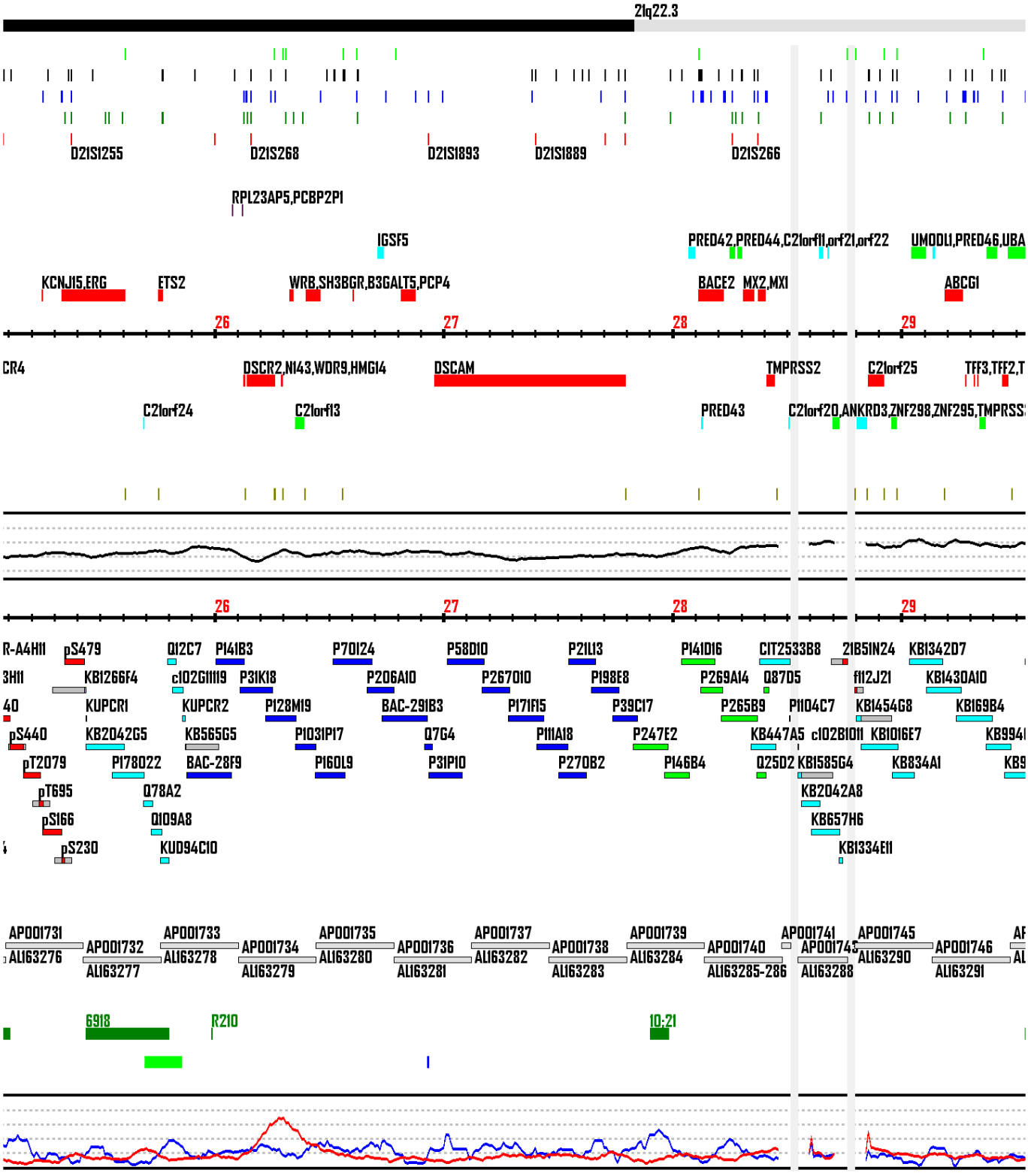

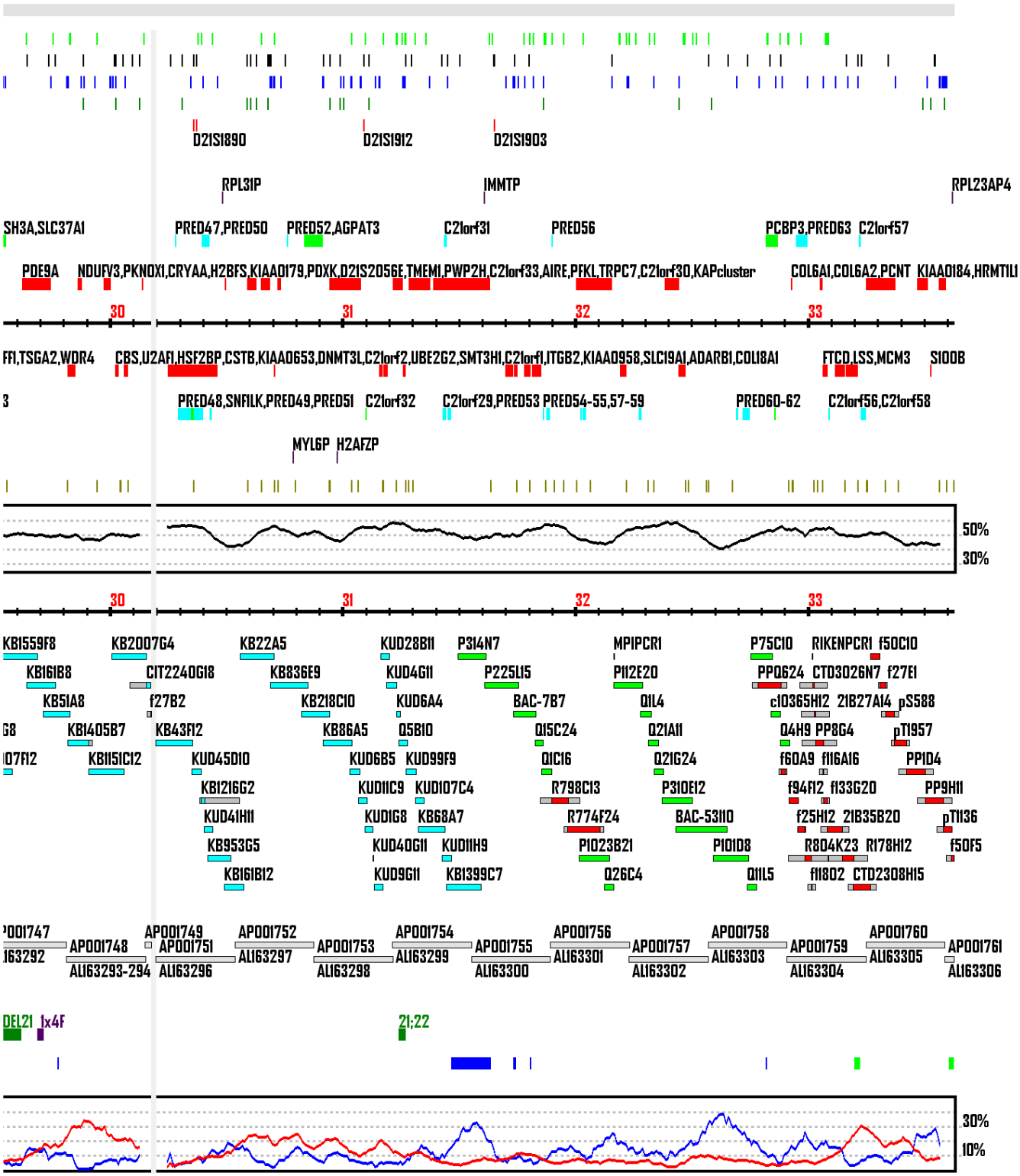

Gene symbol	Accession No		Category	Strand	Position 1	Position 2	Gene size	Genomic clone (s)
TPTE	AF007118	tensin, putative protein-tyrosine phosphatase, EC 3.1.3.48.	1.1	-	425	84293	83869	B15L0C0 + B7L1C4
CYC1LP4		cytochrome c pseudogene	5	-	29708	29866	159	B15L0C0
Pseudo1		putative zinc finger protein pseudogene	5	-	91247	143054	51808	B7L1C4 to pT171+pS39
PRED1		putative gene, protein kinase C ETA type (EC 2.7.1.) like	3.2	-	241159	241231	73	B11L7C8 + pT171+pS39
ORLP1		pheromone receptor pseudogene	5	-	246824	248023	1200	B11L7C8 + pT171+pS39
Pseudo1.1		pseudogene similar to cDNA DKFZp586E1423	5	+	198028	198744	717	B7L1C4 to pT171+pS39
Pseudo2		tubulin tyrosine ligase-like 1 pseudogene	5	+	207391	207760	370	B11L7C8 + pT171+pS39
EIF3S5P		eucaryotic initiation factor-3, subunit 5 pseudogene	5	+	273760	274805	1046	pT171+pS39
Centromere								
PRED65		putative gene with similarity to zinc finger proteins	2.2	-	130521	147341	16821	P133G21
PRED3		putative gene, proto-oncogene protein precursor like	3.1	+	383460	384843	1384	P16C2
PRED4		putative gene with similarities to KIAA1074 and KIAA0565	3.2	-	418462	422157	3696	P16C2 + CIT62L20
ORLP2		pheromone receptor pseudogene	5	+	510692	511506	815	CIT62L20 to P29H4
CNN2P		calponin P pseudogene	5	+	863250	865367	2118	P256M13
C21orf15		spliced EST AJ003450	4.2	-	879683	881808	2126	P256M13
CYP4F3LP		cytochrome P450 pseudogene	5	-	883308	884305	998	P256M13
NF1L1P		neurofibromatosis type 1 pseudogene	5	+	1035710	1043391	7682	B585O4
PRED5		putative gene, lipase (EC 3.1.1.3) like	3.1	-	1218308	1225969	7662	P98L15
RBM11		putative gene, RNA binding motif protein 11 like	3.1	+	1252617	1263937	11321	P98L15 + P90B5
PRED6		putative gene, multidrug resistance associated protein like	3.1	+	1310494	1336235	25742	P98L15 + P90B5
STCH	U04735	human microsomal stress 70 protein ATPase core	1.1	-	1409391	1419705	10315	P90B5 + P126N20
SAMSN-1		gene with homology to KIAA0790 protein	1.2	-	1521779	1582895	61117	P31B5 + CIT39I12
POLR2CP		pseudogene similar to RNA polymerase H subunits	5	+	1794171	1795794	1624	P153I22
NRIP1	X84373	nuclear factor RIP140	1.1	-	1997831	2005069	7239	P30P13 + P270M7
CYC1LP5		cytochrome C pseudogene	5	-	2527156	2527393	238	P75G13 + P265A22
RAD23BLP		UV excision repair protein pseudogene	5	-	2730926	2732615	1690	P111K10
USP25	AF170562	ubiquitin specific protease USP25	1.1	+	2766805	2915540	148736	P111K10 to P135E14
RBPMSLP		RNA-binding protein hermes pseudogene	5	-	2780633	2780945	313	P111K10 + P73M5
C21orf34		spliced EST AA451643	4,1	+	3107948	3267833	159886	R746N6 to R649M24
VDAC2P		voltage-dependent anion channel isoform 2 pseudogene	5	+	3131006	3132089	1084	B746N6 + B783C3
C21orf35		spliced EST AW242517	4.1	+	3524206	3643847	119642	R821P16 + R291N6
C21orf36		spliced EST AA017197	4.2	-	3655580	3655996	417	R291N6
C21orf37		spliced EST N47348	4.2	+	4475612	4485648	10037	R651M22
CXADR	U90716/Y07593	46 kD coxsackievirus and adenovirus receptor (CAR) protein	1.1	+	4549799	4603690	53892	R827P19 + R877L16
BTG3	D64110	B-cell translocation gene	1.1	-	4630458	4649509	19052	R877L16 + R396A17
YG81	AF239726	gene of unknown function, spliced variant EST AI126619	1.1	-	4829991	4856082	26092	P14F16 + pT1545
C21orf39		spliced EST T74237	4.2	-	4872415	4922351	49937	pT1545 + R546A20
RL37P		human ribosomal protein L37 pseudogene	5	+	4930891	4931234	344	R546A20
PRED12		putative gene, membrane protein like	3.1	+	5293260	5297043	3784	P37H21
PRSS7	U09860	human enterokinase; EC 3.4.21.9.	1.1	-	5306124	5440407	134284	P37H21 to R107N17
SLC6A6P		taurine transporter processed pseudogene	5	+	6281763	6283565	1803	R697D18
RL37P2		human ribosomal protein L37 pseudogene	5	+	6631155	6631371	217	R330A3
C1QBPP		human splicing factor 2 hyaluronic acid-binding protein (SF2p32) pseudogene	5	+	6796358	6797194	837	R753B2
C21orf40		spliced EST AA412132	4.2	+	6930543	6937020	6478	R335N5
FDPSP		farnesyl pyrophosphate synthetase processed pseudogene	5	+	7425582	7426142	561	R66B12 + R292N6
KRT18P2		cytokeratin 18 processed pseudogene	5	+	7462183	7463505	1323	R66B12 + R292N6
RPS3AP		ribosomal protein S3 processed pseudogene	5	+	7467697	7468061	365	R66B12 + R292N6
PRED14		human cDNA clone 280692	1.2	-	7780231	7780656	426	R47C12 + R781M3
PPIAP		cyclophilin-related processed pseudogene	5	+	7865216	7865974	759	R781M3
NCAM2	U75330	neural cell adhesion molecule 2 precursor	1.1	+	8232569	8490122	257554	R636L7 to 21B42C4
PRED15		exon prediction only	4,3	+	8576553	8706382	129830	R780G18 to R44J6
PRED16		spliced EST AI188136	4.1	+	9064811	9066584	1774	R745D19
Pseudo3		ETS-like processed pseudogene	5	+	9117241	9118467	1227	R745D19
Pseudo4		ERK3 protein kinase pseudogene	5	+	9385099	9388953	3855	R697O17
ZNF299P		zinc finger-like processed pseudogene	5	+	10039861	10041328	1468	R677J23
EEF1A1P		human elongation factor EF-1-alpha processed pseudogene	5	+	10340314	10341348	1035	R42M17
TUBAP		alpha tubulin (TUBA2) processed pseudogene	5	+	10357546	10359276	1731	R42M17
C21orf53		spliced EST W73844	4.2	-	10936167	10938194	2028	P494A8
RPL13AP		ribosomal protein RPL13A pseudogene	5	+	12311851	12312521	671	CTD2289H10
C21orf42		spliced EST AA442272	4.1	-	12370760	12380055	9296	B2291C14
PRED21		spliced EST AI016585	4.2	-	12532814	12535145	2332	pS11
PRED66		spliced EST N23422	4.1	+	12535700	12549916	14217	pS11
PRED22	AK000458	complete cDNA FLJ20451	1.2	-	12535700	12557525	21826	pS11
C21orf43		gene similar to mouse junctional adhesion molecule, spliced EST AA725566	2.1	-	12633927	12664967	31041	f30F8 + T172
FDXP2		adrenodoxin pseudogene	5	+	12641719	12643723	2005	f30F8
ATP5A	M37104	human mitochondrial ATPase coupling factor 6 subunit	1.1	-	12674543	12684464	9922	pT172
GABPA	U13044, D13318	human nuclear respiratory factor-2 subunit alpha	1.1	+	12685464	12719695	34232	pT172
APP	Y00264	human mRNA for amyloid A4 precursor of Alzheimer's disease	1.1	-	12830594	13120880	290287	pT364 to Q22F1
PRED24		gene similar to MARCKS, cDNA DKFZp564P1664	2.1	-	13177819	13184351	6533	Q22F1 to KB1622E1
ADAMTS1	AF170084	human metalloproteinase with thrombospondin type 1 motifs	1.1	-	13786471	13795380	8910	KB2043D3 + KB126A3
ADAMTS5	NM_007038	disintegrin-like and metalloprotease with thrombospondin type 1 motif, 5	1.1	-	13871628	13916697	45070	KB45E1 + KB1346F10
GPXP2		human glutathione peroxidase (GPXP2) pseudogene	5	-	14093307	14094251	945	KB1411F11
PRED25		exon prediction only	4.3	+	14203290	14213276	9987	KB1411F11 + KB1648B8
EIF4A1P		eukaryotic initiation factor 4AI pseudogene	5	-	14317196	14318136	941	KB1648B8
RPL10P		60S ribosomal protein L10 pseudogene	5	-	14370507	14371248	742	KB1648B8 + KB1987H1
PRED26		exon prediction only	4.3	-	14408249	14439794	31546	KB1987H1
D21S2073		KIAA0253 pseudogene	5	+	14442321	14443123	803	KB1987H1
C21orf23		spliced EST AI796012	4.2	+	14672563	14701383	28821	KB851D4 + KB1919E1
PRED27		exon prediction only	4.3	-	14751587	14796251	44665	KB1919E1 + P50G11
PRED28	AF139682	putative N6-DNA-methyltransferase	1.2	-	15826382	15835617	9236	P273B14 + P886H8
HSPDP7		human chaperonin pseudogene	5	-	15837255	15839603	2349	P273B14 + P866H8
ZNF294	AB018257	human mRNA for KIAA0714 protein	1.2	-	15878401	15943199	64799	P866H8 + P100J12
RPL23P2		60S ribosomal protein L23 pseudogene	5	-	15947825	15948301	477	P100J12
C21orf6		chromosome 21 open reading frame 6	1.1	-	15958389	15969612	11224	P100J12
USP16	AF126736	human ubiquitin processing protease, EC 3.1.2.15.	1.1	+	15974947	16004744	29798	P100J12 + P79E4
CCT8	D13627	T-complex protein 1, theta subunit	1.1	-	16006583	16022451	15869	P100J12 + P79E4
C21orf7		putative gene, TGF-beta-activated kinase like	3.1	+	16079612	16123711	44100	P79E4 + P84N21
GAPDP14		glycerinaldehyde-3-phosphate dehydrogenase pseudogene	5	+	16171147	16172079	933	P84N21
BACH1	A20292	transcription regulator protein	1.1	+	16247722	16294818	47097	P292A20
C21orf12	R82144	spliced EST R82144 (trapped exon)	4.2	-	16318856	16320063	1208	R175P11
C21orf8	AA843704	spliced EST AA843704	4.1	-	16444917	16449219	4303	R175P11
GRIK1	L19058	human glutamate receptor (GLUR5)	1.1	-	16502382	16888900	386519	R32A2 to P209L12
C21orf41		spliced EST N45393	4.1	+	16545371	16546534	1164	R32A2 + c103A0552
C21orf9		spliced EST W58369, nuclear factor	4.2	+	16697787	16712843	15057	R269P7 + 295E05-A
CLDN17	AJ250712	human CLDN17 gene for claudin-17	1.1	-	17114968	17115642	675	R463J19
CLDN8	AJ250711	human CLDN8 gene for claudin-8	1.1	-	17163042	17164972	1931	R463J19
PRED29		exon prediction only	4.3	+	17735491	17830550	95060	R282I5
PRED30		exon prediction only	4.3	+	17840954	17920802	79849	R282I5 + R14B21
UBE3AP2		ubiquitin protein ligase, processed pseudogene	5	-	18009007	18012195	3189	R14B21
TIAM1	U16296	human T-lymphoma invasion and metastasis inducing TIAM1 protein	1.1	-	18069188	18507997	438810	R137B7 to pS158
PRED31		exon prediction only	4.3	+	18401762	18453510	51749	PQ8P9 + pT1040
BTRC2P		pseudogene similar to BTRC	5	+	18576377	18577510	1134	pT650
SOD1	X02317	Cu/Zn superoxide dismutase, EC 1.15.1.1.	1.1	+	18608676	18617893	9218	pS552 + pS322
CTBP2	AF016507	C-terminal binding protein 2	1.1	-	18619970	18650793	30824	pS322 + pPQ119B8
HMG14P		nonhistone chromosomal protein HMG-14 pseudogene	5	+	18655577	18656152	576	pPQ119B8
PRED33		putative serine threonin kinase, homolog to mouse MAK5 AF055919	1.1	+	18822262	18953011	130750	pQ78C10 to pS306
C21orf44		spliced EST AW138869	4.2	-	19029258	19035242	5985	pD5
C21orf45		spliced EST AI369385	4.1	-	19217960	19227693	9734	pT255
KIAA0539	AB011111	human mRNA for KIAA0539 protein	1.2	-	19259964	19290570	30607	pT255 to pD1
PRED34		putative gene, similar to C. elegans P91865, spliced EST H51862	3.2	+	19402248	19464331	62084	pT293 to f1G6
C21orf47		spliced EST H51284	4.2	-	19498020	19498436	417	pT1230
TCP10L		gene similar to TCP10, spliced ESTs AA465232/T18865	2.1	-	19531192	19552136	20945	pT1866
SYNJ1	AF009040	synaptojanin-1, polyphosphoinositide phosphatase	1.1	-	19577707	19649002	71296	pT1866 to pPQ62G5
GCFC	AF153208	human GC-rich sequence DNA-binding factor candidate	1.1	-	19683781	19718831	35051	pT1082 + pS12
C21orf49		spliced EST T19019	4.1	+	19721142	19737649	16508	pS12
PRED36		exon prediction only	4.3	+	19762548	19768318	5771	pS12
PRKCBP2	U48250	human protein kinase C-binding protein RACK17	1.1	+	19975790	19977861	2072	pQ77A10
C21orf54		spliced EST AA934973	4.2	-	20114481	20118775	4295	pQ14E2
IFNAR2	X77722	human interferon alpha/beta receptor	1.1	+	20179027	20211701	32675	pQ95D4 to pS318
IL10RB	Z17227	human transmembrane receptor protein; cytokine receptor	1.1	+	20215375	20246167	30793	pS318
IFNAR1	X60459	human interferon-alpha receptor (HuIFN-alpha-Rec)	1.1	+	20273930	20305504	31575	pD71A4 to PQ38G8
IFNGR2	U05875	interferon-gamma receptor beta chain precursor	1.1	+	20351850	20386468	34619	PQ102G11 + PPACB5
C21orf4	AF045606	chromosome 21 open reading frame 4 (Interferon receptor cluster)	1.2	-	20399658	20428899	29242	PPACB5 to pS590
RPS5L	NM_001009	human ribosomal protein S5 mRNA, complete cds	1.1	+	20430493	20431180	688	pS590
C21orf55		spliced ESTs AA233864/AA232809	4.2	+	20434484	20437154	2671	pS590
GART	X54199	phosphoribosylglycinamide formyltransferase, EC 2.1.2.2.	1.1	-	20452917	20491053	38137	pS590 + pT604
C21orf50		spliced EST AA658915	4.1	+	20492026	20498551	6526	pT604
SON	X63753	SON DNA-binding protein, KIAA1019	1.1	+	20499844	20526435	26592	pT604 + pT377
CRYZL1	AF029689	human quinone oxidoreductase homolog-1	1.1	-	20538571	20590675	52105	pT377 to pT1276
ITSN	AF064243/4	human intersectin-SH3 domain-containing protein SH3P17	1.1	+	20743325	20787448	44124	P130N6 + P201F12
ATP5O	X83218	human ATP synthase OSCP subunit, oligomycin sensitivity conferring protein	1.1	-	20852405	20864736	12332	P149C3
SLC5A3	AF027153	human solute carrier family 5, member 3, Sodium/myo-inositol cotransporter	1.1	+	21022392	21053127	30736	R338L7 + CTD2344F14
PRED37		exon prediction only	4.3	+	21110621	21153303	42683	CTD2344F14 to P245P17
KCNE2	AF071002	human minK-related peptide 1, potassium channel subunit, MiRP1	1.1	+	21319354	21320085	732	pQ12C8
C21orf51		spliced EST AA306264	4.1	+	21328376	21337646	9271	pQ82F5
PRED38		exon prediction only	4.3	+	21368165	21392696	24532	pQ97G8 + pQ45D2
KCNE1	L28168	human cardiac delayed rectifier potassium channel protein	1.1	-	21398192	21398599	408	PPQ336B18
DSCR1	U28833	human Down syndrome candidate region protein, proline-rich protein	1.1	-	21465436	21562791	97356	PPQ125H6 + PPQ31L12
PRED39		exon prediction only	4.3	+	21498407	21524010	25604	PPQ125H6
CLIC1L		putative gene, p64 chloride channel like, spliced ESTs T92523/T91760	3.1	+	21657652	21665430	7779	PPQ140K16
C21orf52		spliced EST AI761253	4.1	-	21672754	21682989	10236	PPQ140K16
RUNX1	D43967	acute myeloid leukemia 1 protein (oncogene AML-1), core-binding factor, alpha subunit	1.1	-	21770223	21837636	67414	PPQ140K16 to P499A22
RPL34P3		pseudogene with similarity to ribosomal protein L34	5	-	22421026	22421405	380	P220P20
RPS20P		pseudogene with similarity to ribosomal protein S20	5	-	22673718	22674176	459	P169K17
PPP1R2P2		protein phosphatase inhibitor 2 pseudogene	5	+	22836211	22837448	1238	c102A0977 + c103C0352
PRED40		exon prediction only	4.3	+	22853397	22921398	68002	c103C0352 to P27A22
RPL23AP3		ribosomal protein L23A pseudogene	5	+	22965074	22965610	537	P27A22
C21orf18		spliced EST AK001660	1.2	-	22983591	23009434	25844	P27A22
RIMKLP		pseudogene for KIAA1238 protein, similar to bacterial ribosomal S6 modification protein	5	+	22999209	23001048	1839	P27A22
C21orf27		spliced EST AI685287	4.2	+	23009481	23013468	3988	P27A22
CBR1	J04056	carbonyl reductase (NADPH) 1, EC 1.1.1.184.	1.1	+	23019072	23022213	3142	P27A22
C21orf19		unspliced ORF	5	+	23079121	23080959	1839	KB795B7
RPS9P		ribosomal protein S9 pseudogene	5	+	23081472	23082155	684	KB795B7
CBR3	AB004854	carbonyl reductase (NADPH) 3, EC 1.1.1.184.	1.1	+	23084242	23095605	11364	KB795B7
C21orf5	AJ237839	chromosome 21 open reading frame 5	1.1	+	23113590	23345278	231689	KB795B7 to KB5G11
RPL3P		ribosomal protein L3 pseudogene	5	-	23117970	23119234	1265	KB795B7
SFRS9P1		splicing factor pseudogene	5	-	23243581	23244505	925	P24J14
RPS26P		ribosomal protein S26 pseudogene	5	-	23252636	23252753	118	P24J14
KIAA0136		human mRNA for KIAA0136 protein	1.1	+	23268980	23325388	56408	P24J14 + KB739C11
CHAF1B	U20980	human chromatin assembly factor-I p60 subunit	1.1	+	23334828	23365571	30744	KB5G11
ATP5J2LP		F1Fo-ATPase synthase f subunit pseudogene	5	-	23337504	23337939	436	KB5G11
CLDN14	AJ132445	human CLDN14 gene	1.2	-	23409717	23410436	720	KB5G11 + KB176G8
PSMD4P		proteasome 26S subunit pseudogene	5	-	23434597	23436159	1563	KB176G8
PRED41		exon prediction only	4.3	+	23498096	23503146	5051	KB176G8 + KB1572B10
SIM2	U80456	human transcription factor SIM2, homolog of the Drosophila single-minded gene SIM1	1.1	+	23648420	23698647	50228	KB594G10
HLCS	D87328	holocarboxylase synthetase, EC 6.3.4.	1.1	-	23699922	23910899	210978	KB594G10 to pD47
DSCR5	AF216305	human Down syndrome critical region protein C	1.1	-	24014111	24021810	7700	KB318C2 to pT1492
TTC3	D84294	tetratricopeptide repeat protein 3 (TPR repeat protein D)	1.1	+	24034533	24151928	117396	pT1212 + pT1601
DSCR3	D87343	Down syndrome critical region protein A	1.1	-	24172248	24216356	44109	pT1601 + pD10
DYRK1A	D86550	dual-specificity tyrosine-Y-phosphorylation regulated kinase, EC 2.7.1.	1.1	+	24367732	24464002	96271	pT1091 to pS165
KCNJ6	U24660	human G protein coupled inward rectifier potassium channel 2 (hiGIRK2)	1.1	-	24573396	24864896	291501	c10C6 to pS611
DSCR4	AB000099	Down syndrome critical region protein B	1.1	-	25002841	25069979	67139	c7A4 to pD40
KCNJ15	Y10745	inwardly rectifing potassium channel Kir4.2.	1.1	+	25245362	25249289	3928	pT695 + pS166
ERG	M17254	transcriptional regulator ERG (transforming protein ERG)	1.1	+	25330315	25609026	278712	pS166 to P178O22
C21orf24		spliced EST AI492145	4.2	-	25687390	25689416	2027	P178O23 + Q78A3
ETS2	J04102	human erythroblastosis virus oncogene homolog 2	1.1	+	25754197	25771822	17626	Q109A8 + KUD94C10
RPL23AP5		60S ribosomal protein pseudogene	5	+	26075948	26076486	539	P141B3
PCBP2P1		heteronucleotide ribosomal protein pseudogene	5	+	26119393	26120517	1125	P141B3 + P31K18
DSCR2	AJ006291	leucine rich protein C21-LRP	1.2	-	26123847	26131838	7992	P141B3 + P31K18
N143	AJ002572	human mRNA; transcriptional unit N143	1.1	-	26142249	26143447	1199	P31K18
WDR9		gene homolog to cAMP response element binding and beta-tranducin family	1.2	-	26144078	26260855	116778	P31K18 + P128M19
HMG14	J02621	human non-histone chromosomal protein HMG-14	1.1	-	26289611	26296346	6736	P128M19
WRB	Y12478	tryptophan-rich protein, congenital heart disease 5 protein	1.2	+	26325991	26343350	17360	P128M19
C21orf13		hypothetical 76.5 kD protein, O95447, myosin heavy chain and kinesin homology	3.1	-	26350852	26389850	38999	P128M19 + P1031P17
SH3BGR	X93498	21-Glutamic Acid-Rich Protein (21-GARP)	1.1	+	26397539	26461157	63619	P1031P17 to P70I24
B3GALT5	AB020337	GlcNAc-beta-1,3-galactosyltransferase 5	1.1	+	26602223	26607784	5562	P70I24
IGSF5		putative gene, immunoglobulin superfamily 5 like	3.1	+	26710455	26737020	26566	P206A10 + BAC-291B3
PCP4	U52969	brain specific polypeptide PEP19	1.1	+	26812439	26874378	61940	BAC-291B3
DSCAM	AF023450	human CHD2-52 down syndrome cell adhesion molecule	1.1	-	26958276	27791902	833627	P31P10 to P39C17
PRED42		exon prediction only	4.3	+	28069946	28098280	28335	P146B4 + P141D16
BACE2	AF050171	beta-site APP-cleaving enzyme 2, EC 3.4.23.	1.1	+	28113408	28221077	107670	P141D16 to P265B9
PRED43		exon prediction only	4.3	-	28124674	28131593	6920	P141D16 + P269A14
PRED44		putative gene containing transmembrane domain	3.1	+	28249038	28271985	22948	P265B9
C21orf11		gene similar to 2-19 protein	2.1	+	28283696	28302461	18766	P265B9
MX2	M30818	human interferon-regulated resistance GTP-binding protein MXB	1.1	+	28307287	28354211	46925	P265B9 + KB447A5
MX1	NM_002462	human interferon-regulated resistance GTP-binding protein MXA	1.1	+	28371509	28404533	33025	KB447A5 to Q87D5
TMPRSS2	U75329	transmembrane protease, serine 2, EC 3.4.21.	1.1	-	28410553	28443714	33162	Q87D5 to CIT2533B8
C21orf20		spliced EST AW138631	4.2	-	28504635	28508473	3839	CIT2533B8
C21orf21		spliced EST AA969880	4.2	+	28638264	28656298	18035	KB2042A8 + KB657H6
C21orf22		spliced EST AA435939	4.2	+	28675954	28676550	597	KB657H6
ANKRD3		putative gene, ankirin like, possible dual-specificity Ser/Thr/Tyr kinase domain	3.1	-	28698345	28726003	27659	KB657H6 + KB1334E11
ZNF298		putative gene containing C2 domain, spliced EST AA490433	3.1	-	28802792	28846674	43883	f112J21 to KB1016E7
C21orf25		human cDNA DKFZp586F0422, AL050173	1.2	-	28852545	28921083	68539	KB1016E7
ZNF295		gene similar to zinc finger 5 protein	2.1	-	28954266	28977792	23527	KB1016E7 + KB834A1
UMODL1		gene similar to uromodulin	2.1	+	29043525	29105067	61543	KB834A1 + KB1342D7
PRED46		exon prediction only	4.3	+	29133888	29143382	9495	KB1342D7 + KB1430A10
ABCG1	X91249	white protein homolog (ATP-binding cassette transporter 8)	1.1	+	29186705	29264680	77976	KB1430A10 + KB169B4
TFF3	L08044	trefoil factor 3, HITF, human intestinal trefoil factor	1.1	-	29279510	29282789	3280	KB169B4
TFF2	X51698	trefoil factor 2, SML1, human spasmolytic polypeptide (SP)	1.1	-	29313816	29318396	4581	KB169B4
TFF1	X00474	trefoil factor, BCE1, human pS2 induced by estrogen from human breast cancer cell line M	1.1	-	29329717	29333970	4254	KB169B4
TMPRSS3		gene similar to transmembrane serine protease	2.1	-	29339326	29363526	24201	KB169B4
UBASH3A		gene similar to UBA containing SH3 domain	2.1	+	29371350	29415100	43751	KB169B4 + KB994G8
TSGA2		human homolog to mouse testis specific gene 2	1.2	-	29439932	29463727	23796	KB994G8 + KB907F12
SLC37A1		gene similar to glycerol-3-phosphate permease	2.1	+	29463525	29549761	86237	KB994G8 to KB1559F8
PDE9A	AF067223	CGMP-specific 3',5'-cyclic phosphodiesterase type 9, EC 3.1.4.17.	1.1	+	29621249	29742945	121697	KB1559F8 to KB51A8
WDR4		WD repeat domain 4	1.2	-	29816661	29846963	30303	KB51A8 + KB1405B7
NDUFV3	X99726/7/8	NADH-ubiquinone oxidoreductase 9 kD subunit precursor, EC 1.6.5.3.	1.1	+	29860728	29876602	15875	KB1405B7
PKNOX1	U68727	human homeobox-containing protein	1.1	+	29971758	29999360	27603	KB1151C12
CBS	L00972	human cystathionine-beta-synthase, EC 4.2.1.22.	1.1	-	30020629	30035840	15212	KB1151C12 + KB2007G4
U2AF1	M96982	human U2 snRNP auxiliary factor small subunit	1.1	-	30060393	30074960	14568	KB2007G4
CRYAA	U05569	human alphaA-crystallin (CRYA1)	1.1	+	30136479	30140239	3761	KB2007G4
HSF2BP	AB007131	heat shock transcription factor 2 binding protein	1.1	-	30249766	30458464	208699	KB953G8
PRED47		exon prediction only	4.3	+	30278845	30283667	4823	KB34F12
PRED48		exon prediction only	4.3	-	30290587	30396599	106013	KB43F12 to KB1216G2
SNF1LK		gene similar to rat protein kinase (KID2)	2.1	-	30346014	30355450	9437	KB43F12 + KUD45D10
PRED49		exon prediction only	4.3	-	30373833	30390064	16232	KUD45D10 + KB1216G2
PRED50		exon prediction only	4.3	+	30394045	30424807	30763	KB1216G2 to KB953G5
PRED51		exon prediction only	4.3	-	30427539	30435071	7533	KUD41H11 + KB953G5
RPL31P		ribosomal protein L31 pseudogene	5	+	30480511	30480915	405	KB953G8
H2BFS	AB041017	H2B histone family S member	1.1	+	30494512	30494892	381	KB953G5 + KB161B12
KIAA0179	D80001	human mRNA for KIAA0179 protein	1.2	+	30588872	30625350	36479	KB22A5
PDXK	U89606	human pyridoxal kinase, EC 2.7.1.35.	1.1	+	30648562	30685351	36790	KB22A5
CSTB	L03558	cystatin B (liver thiol proteinase inhibitor)	1.1	-	30703222	30705637	2416	KB836E9
D21S2056E	U79775	human NNP-1/Nop52 (NNP-1), novel nuclear protein 1	1.1	+	30718866	30733378	14513	KB836E9
PRED52		exon prediction only	4.3	+	30758662	30761538	2877	KB836N9
MYL6P		myosine alkali light chain 6 pseudogene	5	-	30785002	30785646	645	KB836E9
AGPAT3		gene similar to plant lysophosphatidic acid acyltransferase	2.1	+	30833164	30911690	78527	P24J14 to KB218C10
TMEM1	U19252	epilepsy holoprosencephaly candidate-1 protein	1.2	+	30941630	31034013	92384	KB218C10 to KUD6B5
H2AFZP		histone H2AZ pseudogene	5	-	30975252	30976418	1167	KB86A5
PWP2H	X95263	periodic tryptophan protein 2 homolog	1.1	+	31036667	31060455	23789	KB86A5 + KUD6B5
C21orf33	Y07572	human HES1 protein, homolog to E.coli and zebrafish ES1 protein	1.2	+	31062955	31074982	12028	KUD6B5 + KUD11C9
C21orf32		putative gene with similarities to yeast gene YDL038c	3.2	-	31097059	31103123	6065	KUD11C9 + KUD1G8
KIAA0653	AB014553	human mRNA for KIAA0653 protein	1.2	-	31156109	31170220	14112	KUD9G11 + KUD28B11
DNMT3L	AF194032	human cytosine-5-methyltransferase 3-like protein	1.2	-	31175615	31191491	15877	KUD28B11 + KUD4G11
AIRE	Z97990	autoimmune regulator (APECED protein)	1.1	+	31215162	31227494	12333	KUD4G11
PFKL	X15573	human liver-type 1-phosphofructokinase, EC 2.7.1.11.	1.1	+	31229326	31256648	27323	KUD4G11 to Q5B10
C21orf2	Y11392	nuclear encoded mitochondrial protein, cDNA A2-YF5	1.2	-	31258219	31268538	10320	Q5B10
TRPC7	AB001535	transient receptor potential-related channel 7, a novel putative Ca2+ channel protein	1.1	+	31282531	31372356	89826	KUD99F9 to KB68A7
C21orf30		intronless long ORF, AL117578	1.2	+	31389206	31472069	82864	KB68A7 to KB1399C7
C21orf29		spliced partial mRNA	4.2	-	31428574	31440450	11877	KB68A7 + D11H9
C21orf31		spliced EST AJ003549/AJ003550/AJ003554	4.2	+	31436198	31445047	8850	KB68A7 to KB1399C7
PRED53		exon prediction only	4.3	-	31451158	31463198	12041	KUD11H9 + KB1399C7
KAPcluster		keratin associated proteins, gene cluster	see text	see text	31468577	31632094	163518	KB1399C7 to P225L15
IMMTP		motorprotein pseudogene	5	-	31604873	31607494	2622	P314N7
UBE2G2	AF032456	human ubiquitin conjugating enzyme G2	1.1	-	31698366	31731118	32753	P225L15
SMT3H1	X99584	ubiquitin-like protein, a human homolog of the S. cerevisiae SMT3 gene	1.1	-	31734951	31747380	12430	P225L15 + BAC-7B7
C21orf1	Z50022	putative surface glycoprotein C21orf1 precursor	1.1	-	31778924	31803008	24085	BAC-7B7
ITGB2	M15395	cell surface adhesion glycoprotein (LFA-1/CR3/P150,959 beta subunit precursor)	1.1	-	31815297	31850215	34919	BAC-7B7 + Q15C24
PRED54		exon prediction only	4.3	-	31860690	31864574	3885	Q15C24 + Q1C16
PRED55		exon prediction only	4.3	-	31875594	31889131	13538	Q1C16
PRED56		exon prediction only	4.3	+	31896344	31897138	795	Q1C16
ADARB1	U76421	human dsRNA adenosine deaminase DRADA2b, EC 3.5.	1.1	+	32003926	32155953	152028	R774F24 to Q26C4
PRED57		exon prediction only	4.3	-	32021007	32024904	3898	R774F24 + P1023B21
PRED58		exon prediction only	4.3	-	32030142	32044291	14150	R774F24 + P1023B21
KIAA0958	AB023175	human mRNA for KIAA0958 protein	1.2	-	32193331	32217279	23949	P112E20
PRED59		exon prediction only	4.3	-	32273736	32281291	7556	P112E20 + Q1L4
COL18A1	AF018081	human type XVIII collagen	1.1	+	32384934	32443158	58225	P310E12 + BAC-53I10
SLC19A1	U19720	human reduced folate carrier (RFC)	1.1	-	32444153	32471866	27714	P310E12 + BAC-53I10
PRED60		exon prediction only	4.3	-	32690004	32696445	6442	P101D08
PRED61		exon prediction only	4.3	-	32719718	32748256	28539	P101D08 + Q11L5
PCBP3		poly (rC)-binding protein 3	2.1	+	32818086	32868160	50075	P75C10 to PQ624
PRED62		putative gene containing transmembrane domain	3.1	-	32856419	32858945	2527	PPQ624 + c10365H12
COL6A1	X15880	human mRNA for collagen VI alpha-1 C-terminal globular domain	1.1	+	32926714	32931431	4718	f94F12
PRED63		exon prediction only	4.3	+	32949175	32994663	45489	f94F12 to R804K23
COL6A2	X15882	human mRNA for collagen VI alpha-2 C-terminal globular domain	1.1	+	33051649	33059229	7581	PP8G4
FTCD	U91541	human formiminotransferase cyclodeaminase, EC 4.3.1.4.	1.1	-	33062659	33081949	19291	PP8G4 to 21B35B20
C21orf56		spliced EST AA262598	4.1	-	33087542	33087825	284	21B35B20
LSS	D63807	human lanosterol synthase, EC 5.4.99.7.	1.1	-	33114827	33155144	40318	21B35B20 + R178H12
MCM3	AB005543	human mRNA for MCM3 import factor	1.1	-	33161516	33211704	50189	R178H12 + CTD2308H15
C21orf57		spliced EST AI702440	4.1	+	33217793	33224104	6312	CTD2308H15
C21orf58		spliced ESTs Z25278/AA825266	4.1	-	33227047	33244524	17478	CTD2308H15
PCNT	U52962	pericentrin, kendrin (KIAA0402)	1.1	+	33250559	33372115	121557	CTD2308H15 to pT1957
KIAA0184	D80006	human mRNA for KIAA0184 protein	1.2	+	33468225	33511361	43137	pT1957 + PP1D4
S100B	M59488	S-100 calcium-binding protein, beta chain	1.1	-	33524582	33525899	1318	PP9H11
HRMT1L1	X99209	protein arginine N-methyltransferase 2, EC 2.1.1.	1.1	+	33562032	33591323	29292	PP9H11 + pT1136
RPL23AP4		ribosomal protein L23A pseudogene	5	+	33617159	33617631	473	f50F5